Progenitor potential of *nkx6.1*-expressing cells throughout zebrafish life and during beta cell regeneration

Aurélie P. Ghaye[1*], David Bergemann[1*], Estefañía Tarifeño-Saldivia[1], Lydie C. Flasse[1], Virginie Von Berg[1], Bernard Peers[1], Marianne L. Voz[1**§] and Isabelle Manfroid[1**§]

[1] Laboratory of Zebrafish Development and Disease Models (ZDDM), GIGA-Research, Avenue de l'Hôpital 1, B34, 4000 Liège (Sart-Tilman), University of Liège Belgium

[*] and [**] These authors contributed equally to this work

[§]Corresponding authors

Email addresses:

APG: aurelieghaye@outlook.be
DB: david.bergemann@student.ulg.ac.be
ETS: etarifeno@student.ulg.ac.be
LCF: lydie.flasse@sund.ku.dk
VVV: vonbergvirg@hotmail.com
BP: bpeers@ulg.ac.be
MLV: mvoz@ulg.ac.be
IM: isabelle.manfroid@ulg.ac.be

Abstract

Background: In contrast to mammals, the zebrafish has the remarkable capacity to regenerate very efficiently its pancreatic beta cells. Understanding the mechanisms of regeneration in zebrafish and the differences with mammals will be fundamental to discovering molecules able to stimulate the regeneration process in mammals. To identify the pancreatic cells able to give rise to new beta cells in zebrafish, we generated new transgenic lines allowing the tracing of multipotent pancreatic progenitors and endocrine precursors.

Results: Using novel bacterial artificial chromosome transgenic *nkx6.1* and *ascl1b* reporter lines, we established that *nkx6.1*-positive cells give rise to all the pancreatic cell types and *ascl1b*-positive cells give rise to all the endocrine cell types in the zebrafish embryo. These two genes are initially co-expressed in the pancreatic primordium and their domains segregate, not as a result of mutual repression, but through the opposite effects of Notch signaling, maintaining *nkx6.1* expression while repressing *ascl1b* in progenitors. In adult zebrafish, *nkx6.1* expression persists exclusively in the ductal tree at the tip of which its expression coincides with Notch active signaling in centroacinar/terminal end duct cells. Tracing these cells reveals that they are able to differentiate into other ductal cells and into Insulin-expressing cells in normal – non-diabetic – animals. This capacity of ductal cells to generate endocrine cells is supported by the detection of *ascl1b* in the *nkx6.1*:GFP ductal cell transcriptome. This transcriptome also reveals, besides actors of the Notch and Wnt pathways, several novel markers such as *id2a*. Finally, we show that beta cell ablation in adult zebrafish triggers proliferation of ductal cells and their differentiation into Insulin-expressing cells.

Conclusions: We have shown that, in the zebrafish embryo, *nkx6.1*+ cells are *bona fide* multipotent pancreatic progenitors, while *ascl1b*+ cells represent committed endocrine precursors. In contrast to mouse, pancreatic progenitor markers *nkx6.1* and *pdx1* continue to be expressed in adult ductal cells, a subset of which we show are still able to proliferate and undergo ductal and endocrine differentiation, providing robust evidence of the existence of pancreatic progenitor/stem cells in adult zebrafish. Our findings support the hypothesis that *nkx6.1*+ pancreatic progenitors contribute to beta cell regeneration. Further characterization of these cells will open up new perspectives for anti-diabetic therapies.

Keywords

nkx6.1, ascl1, pancreas, duct, centroacinar cells, beta cells, stem cells, lineage tracing, multipotent progenitors, regeneration, diabetes, zebrafish, Notch, Wnt

Background

The pancreas is composed of an exocrine compartment with acinar and ductal cells, which secrete and transport digestive enzymes into the gut, and an endocrine compartment, which regulates glucose homeostasis by secreting pancreatic hormones into the bloodstream. Loss of pancreatic Insulin-producing cells (beta cells) is a hallmark of diabetes. An attractive therapeutic approach to cure this disease is to stimulate beta cell regeneration *in vivo* from another pancreatic cell type or from progenitors. However, the regenerative capacity of beta cells is very limited in mammals and the cellular and molecular mechanisms involved need to be well understood before being able to stimulate this process. The zebrafish (*Danio rerio*), owing to its phenomenal capacity to restore beta cells after targeted cell ablation [1-3], has become an attractive model organism for the study of the regeneration process. To this end, tools need to be developed, especially to define the source of the new beta cells. So far, no zebrafish transgenic lines have been available to allow a lineage tracing of either multipotent pancreatic progenitors, giving rise to both exocrine and endocrine tissues, or pancreatic endocrine precursor cells.

Pancreas develops from two domains, called the dorsal bud and the ventral bud, which emerge from the foregut endoderm [4, 5]. In zebrafish, the dorsal bud generates the first wave of endocrine cells which cluster at 24 hours post-fertilization (hpf) to form the principal islet [6]. The ventral bud emerges anteriorly to the dorsal bud at 32 hpf and gives rise to acinar, ductal, and to a second wave of endocrine cells [4, 7, 8]. These late endocrine cells originate either from the extra-pancreatic ducts (EPD) and contribute to the expansion of the principal islet [9-11] or from the intra-pancreatic ducts (IPD) and form small secondary islets all along them. These IPD contain pancreatic Notch-responsive cells (PNCs) which represent a population of progenitors of endocrine cells and ductal cells but not of acinar cells [7, 12].

Notch signaling pathway controls the differentiation of pancreatic cells both in zebrafish and mice (reviewed by [13]). One of its functions is to maintain a pool of progenitors in an undifferentiated state through the repression of genes of the achaete scute-like (ASCL) family or of the atonal-related protein (ARP) family. In the murine pancreas, Notch signaling prevents endocrine cell differentiation through the repression of *neurog3* [14]. In zebrafish, *neurog3* is not expressed in the pancreas and therefore the control of endocrine cell fate is fulfilled by other ASCL/ARP factors, namely Ascl1b and Neurod1, which are both repressed by Notch signaling [15]. Exactly like the inactivation of murine *Neurog3*, their simultaneous inactivation completely prevents endocrine cell differentiation leading to

the loss of all hormone-secreting cells [15]. *ascl1b* is the earliest pancreatic marker identified during zebrafish development, its expression starting at the end of gastrulation in the prospective pancreatic region (10 hpf). *ascl1b* is transiently expressed during the formation of the dorsal bud (from 10 hpf to 17 hpf) and, like murine *Neurog3*, is not detected in hormone-expressing cells. Later, in the ventral bud, *ascl1b* expression is turned on when the endocrine cell differentiation program is induced through the blocking of Notch signaling [7, 12, 16]. This Notch inactivation triggers a massive expression of *ascl1b* in the IPD [15]. These data suggest that *ascl1b* expression is restricted to the committed endocrine precursors. However, the observation that the onset of *ascl1b* expression in the prospective pancreatic region precedes all other known pancreatic progenitor markers raises the possibility of the multipotency of the first *ascl1b*+ cells.

Another key factor for pancreatic development is the homeobox transcription factor Nkx6.1. In mouse, it is expressed in the multipotent progenitors during early pancreatic development [17], and, in zebrafish, *nkx6.1* is expressed early in the pancreatic primordium of the dorsal bud (from 11.5 hpf onwards) [18]. At later developmental stages in the mouse embryo, *Nkx6.1* becomes restricted to the endocrine/duct bipotential trunk domain [19]. Similarly, *nkx6.1* is first broadly expressed in the zebrafish pancreatic ventral bud primordium [20], then segregates from the *ptf1a*+ acinar cells to persist in the primitive ducts [20-22] that will give rise to the mature ducts and to secondary islets [7]. In mouse, *Nkx6.1* is expressed in the differentiated beta cells [23] while in zebrafish, *nkx6.1* is never expressed in beta cells nor in the other pancreatic hormone expressing cells [18]. These data suggest that in zebrafish *nkx6.1* also marks multipotent pancreatic progenitors. However, previous findings suggested that the early ventral bud primordium was composed of a heterogeneous population of pancreatic cells composed of Notch-responsive cells, giving rise to ductal and endocrine cells, separated from the *ptf1a*+ cells which generate the acinar cells [7]. This study raises the question of the identity of the multipotent pancreatic progenitors in the zebrafish ventral pancreatic bud and its derivatives.

Here, we show that *nkx6.1* labels multipotent pancreatic progenitors giving rise to all of the different pancreatic cell types (endocrine, ductal, and acinar) while *ascl1b* marks endocrine precursors leading to the different endocrine cell types. For this purpose, we have generated two novel BAC transgenic *nkx6.1* and *ascl1b* reporter lines, *Tg(nkx6.1:eGFP)* and *Tg(ascl1b:eGFP-2A-creER^{T2})*, that both faithfully recapitulate the expression of the *nkx6.1* and *ascl1b* endogenous genes. Using these novel transgenic tools, we were able to analyze in detail the interdependency between these two factors and their relationship with Notch signaling pathway. We also demonstrate that *nkx6.1* expression persists in the adult ductal

tree, notably in the centroacinar/terminal end duct cells, for which we show that they are able to differentiate into Insulin-expressing cells *in vivo*. By isolating *nkx6.1:*eGFP+ cells from dissected pancreas of adult fish, we determined the transcriptome of adult pancreatic ductal cells, which revealed the expression of several regulatory genes potentially involved in endocrine regeneration. Finally, we provide evidences that regenerating beta cells also originate from ductal cells.

Results

The bacterial artificial chromosome reporter *Tg(nkx6.1:eGFP)* recapitulates *in vivo* the expression of the endogenous *nkx6.1* gene

To label the *nkx6.1*-expressing cells, we generated a transgenic line driving the expression of the enhanced green fluorescent protein (eGFP) under the control of *nkx6.1* regulatory regions. We engineered a bacterial artificial chromosome (BAC) spanning from 55 kb upstream to 95 kb downstream of the *nkx6.1* gene and inserted the eGFP coding regions into the exon 1, replacing the beginning of the *nkx6.1* open reading frame (Additional file 1: Figure S1A). This BAC reporter construct was introduced into the zebrafish genome using the Tol2 transposon system [24, 25] and the stable transgenic line *Tg(nkx6.1:eGFP)* obtained showed expression of GFP in the nervous system and in the pancreas, which mirrors the endogenous Nkx6.1 protein expression (Additional file 1: Figure S1B). Detailed comparison of the localization of these two proteins in the pancreas during development confirmed that the GFP protein is indeed co-expressed with Nkx6.1 (Figure 1). Indeed, together with the endogenous Nkx6.1 protein [18], GFP is expressed at the base of the endocrine islet at 24 and 30 hpf (Figure 1B-C), in the ventral bud at 38 hpf and 48 hpf (Figure 1D-E), and in the intra-pancreatic (IPD) and extra-pancreatic (EPD) ducts at 4 dpf (Figure 1F, F'). In contrast, at earlier stages, GFP was detected in a subset of Nkx6.1+ cells, probably due to the delay of GFP expression compared to Nkx6.1. Indeed, at 17 hpf, about 75% of the Nkx6.1+ cells showed detectable GFP expression (Figure 1A, A') and at 14 hpf, this proportion dropped even further to about 25-30% (data not shown). Conversely, a few hours after the onset of *nkx6.1* gene expression, some GFP+/Nkx6.1- cells were also detected (green arrows, Figure 1B'-E'). This GFP labeling is not the result of an ectopic expression of the *gfp* transcript as double fluorescent whole-mount in situ hybridization showed that the *gfp* transcripts are present in the same pancreatic domain as *nkx6.1* transcripts (data not shown) and importantly, like *nkx6.1*, *gfp* transcripts were not found in hormone expressing cells (Additional file 1: Figure S1C-C'' and D-D''). Hence, prolonged GFP detection is rather due to the well-known high stability of the GFP protein (± 24 h half-life [26]) which persists in cells

where Nkx6.1 protein is no longer found. This is nicely illustrated at 30 hpf, where strong GFP expression is detected at the base of the forming islet where Nkx6.1+ pancreatic progenitors are located, while weak GFP labeling is found dorsally within the islet, where differentiated endocrine cells, devoid of Nkx6.1, are clustered (Figure 1C). As expected, this prolonged GFP detection will gradually fade away to finally completely disappears in the differentiated endocrine cells (see Figure 1F).

The high stability of the GFP protein allowed us to perform short-term lineage tracing studies to follow the immediate progeny arising from *nkx6.1*+ cells.

nkx6.1 **expressing cells are multipotent progenitors giving rise to all pancreatic cell lineages**

By short-term lineage tracing studies, we first assessed if *nkx6.1*+ cells can give rise to the first wave of endocrine cells of the dorsal bud using the *Isl1* marker which labels all mature endocrine cells. In contrast to the endogenous *nkx6.1* and the *nkx6.1:GFP* transcripts, which are not co-expressed with *isl1* ([18] and Additional file 1: Figure S1D-D''), GFP was detected in 40 ± 3.8% of Isl1+ cells in *Tg(nkx6.1:eGFP)* embryos (n=10) at 30 hpf indicating that *nkx6.1* cells can give rise to endocrine cells (Figure 2A-A''). Also, we found GFP in all different endocrine cell types, i.e. in 35 ± 18.8% of Insulin+ (Ins) cells (n=21) (Figure 2B-B''), 42 ± 12.5% Somatostatin+ (Sst) cells (n=4) (Figure 2C-C''), and 77 ± 3.7% of Glucagon (Gcg) cells (n=5) (Figure 2D-D''). The percentage of GFP+ cells in the different endocrine subtypes appeared to depend on the onset of expression for each hormone, which is from 15 hpf onward for *ins*, 17 hpf for *sst2* and 21 hpf for *gcga*. Therefore, when the first hormone-expressing cells differentiate from the pool of *nkx6.1*+ progenitors, only a minority of them have accumulated enough GFP to be detected, as explained above (see Figure 1A and data not shown).

Next, we analyzed whether the *nkx6.1*+ cells also contribute to the cells originating from the ventral bud (ductal, acinar, and secondary islets). With Nkx6.1 being expressed in all pancreatic ductal cells (as shown in Figure 1E), we detected accordingly an expression of GFP in all pancreatic ducts labeled by 2F11 antibody (Figure 2F, F'). In contrast, while endogenous *nkx6.1* never co-localizes with *trypsin* (data not shown), a marker of mature acinar cells, GFP was detected in a large majority of acinar cells at 55 hpf (70 ± 25% of *trypsin*+ cells (n=8)), the stage when acinar cells have just begun to differentiate (Figure 2E, E'). Here again, the prolonged GFP detection in the acinar cells gradually disappears and, from 3 dpf, the acinar cells are no more labeled with GFP (shown at 5 dpf in Figure 2F'). And finally, to determine whether *nkx6.1*+ cells can give rise to the secondary islets, emerging from the intrapancreatic ducts, we treated *Tg(nkx6.1:eGFP)* larvae with the Notch-signaling

inhibitor LY411575 from 3 to 5 dpf in order to increase the number of late endocrine cells and thereby facilitate their detection [7, 12, 16]. In LY411575-treated larvae, we observed an increase of the endocrine cells in the principal islet and the appearance of numerous endocrine cells in the pancreatic tail (yellow arrows, Figure 2H, H'), as previously reported. All these endocrine cells are co-labeled with GFP (n=4) indicating that the *nkx6.1*+ ductal cells can also give rise to the secondary islets.

These data indicate that *nkx6.1*-expressing cells are multi-lineage pancreatic progenitors which can differentiate into endocrine, acinar, and ductal cells.

ascl1b-expressing cells give rise exclusively to the endocrine lineage

In order to determine whether *ascl1b* is expressed in the multipotent pancreatic progenitors or in the endocrine precursors, we determined the cell fate of the *ascl1b*-expressing cells. To that end, a BAC reporter *Tg(ascl1b:eGFP-2A-creER^{T2})* was engineered where the bicistronic transcript *eGFP-2A-creER^{T2}* is under the control of the promoter and regulatory sequences of *ascl1b*. Thus, we replaced the beginning of the *ascl1b* open reading frame with an *eGFP-2A-creER^{T2}*cassette (Additional file 2: Figure S2A). The expression profile of GFP in the stable transgenic line *Tg(ascl1b:eGFP-2A-creER^{T2})* faithfully recapitulates the expression of the endogenous *ascl1b* transcript (Additional file 2: Figure S2B-D).

Cell fate experiments were performed by Cre/loxP-based lineage tracing approaches by crossing the *Tg(ascl1b:eGFP-2A-creER^{T2})* with Cre-responder transgenic lines, either *Tg(ubi:loxP-AmCyan-loxP-ZsYellow)*, termed *Tg(ubi:CSY)* [27], or *Tg(ubi:loxP-eGFP-LoxP-mCherry)*, termed *Tg(ubi:Switch)* [28] (Figure 3A). The double-transgenic embryos were treated five times with 4-hydroxytamoxifen (4OH) from 11 to 15 hpf, the period when *ascl1b* expression reaches its maximal level [15], and the embryos were analyzed at 48 or 72 hpf. With these five 4OH treatments, many *ascl1b*-expressing cells have undergone CRE recombination while no recombination was detected in the treated single-transgenic embryos used as control (data not shown). The CRE-mediated recombination marker (Rec Marker standing for either ZsYellow or mCherry) analyzed in double-transgenic embryos at 48 hpf was detected in 38 ± 4.3% of Isl1+ cells(n=5), indicating that *ascl1b*+ cells give rise to the endocrine cells of the dorsal bud (Figure 3B-B''). In a similar way, the Rec Marker was detected in 58 ± 7.1% of the Ins+ cells (n=9) (Figure 3C-C'') and in 59 ± 3.7% of the Gcg+ cells (n=9) (Figure 3D-D''). In contrast, the Rec Marker, clearly visible in the endocrine islet, was not detected at 72 hpf in the ductal cells, labeled by Nkx6.1, nor in the acinar cells, which surround them (Figure 3E, E'), indicating that *ascl1b*+ cells cannot give rise to exocrine cells. Finally, we determined whether the *ascl1b*+ cells give rise to the secondary islets emerging from the intrapancreatic ducts, either artificially induced by inhibiting the Notch

pathway or naturally occurring in 20 dpf larvae. As the combined treatment of LY411575 with 4OH was lethal, we performed short-term lineage tracing based on GFP expression (instead of Cre/loxP-based lineage tracing analyses). As shown in Figure 3F-G, LY411575 treatment from 3 to 5 days of the *Tg(ascl1b:eGFP-2A-creER^{T2})* larvae led to the appearance of GFP cells all along the IPD, most of these cells being also positive for Glucagon or Insulin hormones (yellow arrows, Figure 3G, G'), indicating that *ascl1b*+ cells give rise to induced secondary islets. In order to trace the naturally occurring endocrine cells, we treated *Tg(ascl1b:eGFP-2A-creER^{T2}); Tg(ubi:Switch)* larvae with 4OH at 13, 14 and 17 dpf and analyzed the larvae at 20 dpf. The Rec Marker was detected within the principal islet (Figure 3H, H') as well as in secondary islets (Figure 3I, I') confirming that *ascl1b*+ cells can give rise to secondary islets.

In conclusion, our data demonstrate that *ascl1b*+ cells exclusively give rise to the endocrine cells originating from both dorsal and ventral bud.

nkx6.1 and _ascl1b_ are first co-expressed in the endocrine precursors of the dorsal bud but rapidly their expression domain segregates

As presented above, *nkx6.1* is expressed in the multipotent pancreatic progenitors and *ascl1b* in the endocrine precursors; we therefore analyzed the relationship between these two populations by comparing the Nkx6.1 and GFP proteins in *Tg(ascl1b:eGFP-2A-creER^{T2})* embryos. At 14 hpf, the *ascl1b*:eGFP cells delineate two lines adjacent to the midline (Figure 4A-A''). These cells correspond to the most medial endodermal cells (indicated by M in Figure 4A'), reported to give rise mostly to pancreatic endocrine cells [29, 30]. At this stage, all of these *ascl1b*:eGFP cells also express Nkx6.1. In contrast, the Nkx6.1 expression domain is larger and, in addition to its expression in the hypochord (indicated by H in Figure 4A), it is also expressed in the lateral cells, reported to give rise to exocrine and intestinal cells [29]. Rapidly, these two domains segregate as, as early as 1 hour later, the majority of *ascl1b:e*GFP+ cells no longer express Nkx6.1 (Figure 4B-B''). Thus, separation of the two domains is largely completed when hormone-expressing cells start differentiating.

To determine whether such segregation results from a mutual repression, we examined whether the loss of *ascl1b* leads to an increase of *nkx6.1* expression and vice versa. We generated *ascl1b* and *nkx6.1* loss-of-function mutants using the CRISPR/cas9 genome editing technology [31] (see the Methods section and Additional file 3, Figure 3A, A' and Additional file 4, Figure 4A, A'). As shown in Figure S3 (see Additional file 3), the loss of *ascl1b* does not affect the expression of *nkx6.1* (Figure S3D-E) while it significantly reduces the number of *sst2*+ cells (Additional file 3: Figure S3B-C), as reported for the *ascl1b* morphants [15]. In the same way, *ascl1b* expression does not increase in *nkx6.1* loss-of-function mutant embryos (Additional file 4: Figure S4F-G) for which the effective loss of

nkx6.1 expression was confirmed by immunodetection of Nkx6.1 (Additional file 4: Figure S4B-C) and by the drastic reduction in the number of Gcg+ cells (Additional file 4: Figure S4D-E), as reported for the *nkx6.1* morphants [18].

ascl1b and _nkx6.1_ are regulated in an opposite way by Notch signaling pathway

We then tested whether the segregation of *ascl1b* and *nkx6.1* expression domains results from a different response to the Delta/Notch signaling pathway. To analyze the impact of Notch signaling on *nkx6.1* and *ascl1b* expression, we performed Notch loss- and gain-of-function analyses. We first analyzed the expression of *nkx6.1* and *ascl1b* in mind bomb mutants (*mib*^{ta52b}) in which Notch signaling is disrupted [32]. As previously reported [15], expression of *ascl1b* is strongly increased in *mib* embryos at 15 hpf (Figure 5A-B), in both pancreas and the nervous system. The opposite effect was observed for *nkx6.1* whose expression is reduced at the same stage (Figure 5C-D) and completely lost at 18 hpf (Figure 5E-F). This suggests that Notch signaling pathway is essential for maintaining *nkx6.1* expression but not for its initiation. This was confirmed by the finding that, at 13 hpf, *nkx6.1* expression was unchanged in *mib* mutants while *ascl1b* was already upregulated (Additional file 5: Figure S5A-D).

The same conclusion was drawn for the ventral bud where 3 to 5 dpf treatment with the LY411575 Notch inhibitor led to a complete loss of Nkx6.1 expression and a drastic increase of *ascl1b*:eGFP at 5 dpf (Figure 5G-H). Similar to the dorsal bud, the initiation of *nkx6.1* expression in the ventral bud is not dependent on Notch signaling as its expression at 34 hpf was not perturbed in the *mib* mutant (Additional file 5: Figure S5E-F).

For gain-of-function approaches, we crossed the *Tg(hsp70:Gal4)* with *Tg(UAS:NICD)* [33] and heat-shocked the embryos at 11 hpf to overexpress the Notch intracellular domain (NICD). At 3 hours after the heat-shock, we observed a complete loss of *ascl1b* expression (Figure 5I-J) concomitant with an increase of *nkx6.1* in the NICD overexpressed embryos (Figure 5K-L). This increase was even more important at 30 hpf, when a drastic expansion in the number of *nkx6.1*+ cells was observed in the embryos overexpressing NICD (Figure 5N) compared to the control (Figure 5M).

In conclusion, these data show that Notch signaling represses *ascl1b* expression while it is essential for maintaining *nkx6.1* expression. By contrast, the initiation of *nkx6.1* expression is independent of Notch activity, both in the dorsal and the ventral buds.

Most, but not all, Nkx6.1+ cells are Notch-responsive cells

nkx6.1 being dependent on Notch signaling for maintaining its own expression, this prompted us to compare the location of the Notch-responsive cells and the Nkx6.1+ cells using the *Tg(Tp1:VenusPest)* [16] or *Tg(Tp1:eGFP)* [12] lines in which fluorescent markers

are under the control of Notch-responsive elements (*Tp1*). In the prospective dorsal bud, we could detect Venus labeling in a subset of Nkx6.1 cells at 14 hpf (Figure 6A, A') while 3 hours later (17 hpf), Venus was found in the vast majority of Nkx6.1+ cells (Figure 6B, B'). Similarly, at the beginning of the formation of the ventral bud (38 hpf), only a subpopulation of Nkx6.1+ cells present some Notch activity (Figure 6C, C') while at 65 hpf, the vast majority of Nkx6.1+ cells show Notch activity with the exception of the EPD anlagen (Figure 6D, D'), known to be Notch inactive [34]. At 4 days, virtually all Nkx6.1+ cells are Notch-responsive in the IPD (but the EPD is still devoid of Notch activity) (Figure 6E, E').

In conclusion, these observations indicate that, in both dorsal and ventral buds, *nkx6.1*+ cells progressively acquire Notch signaling activity, essential to maintain *nkx6.1* expression.

nkx6.1 expression persists in ductal cells in the pancreas of adult zebrafish

We then wished to characterize *nkx6.1* expression in pancreas of adult zebrafish. Immunodetections on paraffin sections through the pancreas of 6 to 9 month-old *Tg(nkx6.1:eGFP)* fish revealed that *nkx6.1*:eGFP expression persists in adult zebrafish (Figure 7A). Comparison of endogenous Nkx6.1 protein and GFP shows that, in the adult too, *Tg(nkx6.1:eGFP)* recapitulates the pattern of Nkx6.1 expression (data not shown). *nkx6.1*:eGFP expression is confined to the ducts and to isolated cells scattered throughout the exocrine tissue and was not detected in beta cells (Figure 7A-A') or acinar cells. These *nkx6.1*:eGFP+ cells dispersed within the exocrine pancreas exhibit long cellular extensions characteristic of centroacinar/terminal end duct cells (CACs) (inset in Figure 7A) [12]. In the adult zebrafish pancreas, as in mammals, the CACs can also be identified by Notch signaling activity [12]. Thus, to confirm the expression of *nkx6.1* in CACs, we used the Notch reporter line *Tg(Tp1:VenusPest)* [16], in which the destabilized Venus fluorescent protein (VenusPest) highlights cells harboring ongoing Notch activity, and which labels the CACs, as expected (Figure 7B and inset). All Venus+ cells in the pancreas were found exclusively in the ductal system, and more particularly in the CACs and not within the ductular structures (Additional file 6: Figure S6). Comparison of Venus with Nkx6.1 confirmed that Nkx6.1 is indeed expressed in all Venus+ CACs (Figure 7C-C'). In contrast, while ducts also display *nkx6.1* expression as revealed with either *nkx6.1*:eGFP (Figure 7A-A') or with the endogenous Nkx6.1 protein (Figure 7D), they are devoid of Notch ongoing activity (white arrows pointing at Venus- ducts in Figure 7B, 7D, see also Figure 8A and Additional file 6: Figure S6).

Adult centroacinar cells display progenitor capacity in physiological condition

We then asked whether CACs could generate other pancreatic cell types in adult zebrafish under physiological conditions by using the double *Tg(Tp1:VenusPest); Tg(Tp1:H2BmCherry*) in which the stable H2BmCherry protein labels cells harboring ongoing Notch activity (Venus+ mCherry+) and cells having previously experienced Notch activity (Venus- mCherry+) [16]. This tool has been previously exploited to characterize and follow the fate of the Notch-responsive progenitors in the IPD of larvae [16, 35]. We thus characterized the Venus- H2BmCherry+ cells in adult fish to identify the pancreatic cell types derived from CACs. In about 30% of all H2BmCherry+ cells, Notch activity was switched off (Venus-). Many of these cells, with weak H2BmCherry labeling, were identified within small ducts (Figure 8A-C) that can be identified by the ductal marker 2F11 (Figure 8B-C and Additional file 7: Figure S7A-C for the separated colors and additional example) [11, 22, 36] or by Nkx6.1 (Additional file 7: Figure S7D), and at the tip of which reside CACs (intense H2BmCherry, asterisk in Figure 8C and Additional file 7: Figure S7). Furthermore, low levels of H2BmCherry were also identified in some Insulin-expressing cells (Figure 8D-D'). About 4.9 ± 2.6 % (n=4) of the H2BmCherry+/Notch OFF (Venus-) display Ins labeling. These findings show that mCherry+ terminal end duct cells and Insulin-expressing cells originate from Notch positive CACs. Overall this reveals that a subset of the Nkx6.1+ ductal cells, the Notch-responsive CACs, can generate ductal and endocrine cells.

To determine the capacity of CACs to replicate, their proliferative status was analyzed using EdU labeling and PCNA immunodetection in *Tg(Tp1:VenusPest)* adult fish. One day after EdU injection, a small fraction of CACs (5.8 ± 2.6%, out of 600 counted CACs) had incorporated EdU. All these EdU+ Venus+ cells also express the proliferation marker PCNA (Figure 8E-E'). In contrast, five days post injection, Venus+ cells that still display EdU labeling were no longer PCNA+ (Figure 8F-F'), but still harbor characteristics of CACs, suggesting that they became post-mitotic CACs. The capacity of CACs to replicate together with their ability to undergo ductal and endocrine differentiation indicate that they can behave as adult pancreatic progenitor/stem cells *in vivo*.

***nkx6.1*-expressing ductal cells contribute to beta cell regeneration in adult zebrafish**

The capacity of CACs to differentiate into beta cell in the normal adult zebrafish raises the question whether similar plasticity exists in condition of regeneration. To induce beta cell regeneration, we used the *Tg(ins:NTR-mCherry)* line [1] and treatment with metronidazole (MTZ). The metronidazole is converted into a cytotoxic compound by the Nitroreductase enzyme (NTR) which thereby triggers selective beta cell death by apoptosis [3]. In adult zebrafish, the ablation of beta cells causes dramatic hyperglycemia within 3 days rapidly followed by spontaneous normalization within 2 weeks and beta cell regeneration [2]. To

analyze the ductal cells in the setting of beta cell regeneration, *Tg(nkx6.1:eGFP); Tg(ins:NTR-mCherry)* adult fish were treated with MTZ (day 1) and sacrificed at different time points during regeneration to analyze GFP and Ins on tissue sections at the level of the principal islet. The blood glucose level was measured just before sacrifice. At 3 dpt, ablation was total and effective as reported [2, 37]. MTZ-treated fish displayed severe hyperglycemia as expected (> 500 mg/dl, n=10 fish) while the glycemia of non-treated (CTL) fish was at normal values of 61 ± 19 mg/dl (n=11). Immunolabeling at 3 dpt indicated total beta cell ablation as manifested by the absence of Insulin staining in the pancreas of MTZ-treated *Tg(nkx6.1:eGFP); Tg(ins:NTR-mCherry)* fish (Figure 9A-B). At 9 dpt, first new beta cells have started to re-appear (Figure 9C). Glycemia was still above normal values but nonetheless decreased (145 ± 31 mg/dl, n=2). The principal islet in the treated fish still showed very weak Insulin expression but a few new beta cells (about 5% of the islet cells, compared to 40 to 70% in control fish) can be detected in the principal islet as well as throughout the exocrine tissue as isolated cells or as small clusters of Ins-expressing cells next to CACs and ductal cells marked by GFP (Figure 9C, yellow arrows). The presence of Insulin-expressing cells at 9 dpt is indicative of beta cell regeneration. Interestingly, some of the regenerating Insulin+ cells displayed weak GFP staining (7.9 ± 3.2 % of the Ins+ cells, 452 counted cells, n=2 fish) (Figure 9F). These cells were found next to strongly GFP-labeled ductal nkx6.1:eGFP cells. GFP+ Ins+ cells were also detected at 21 dpt (11.1 ± 4.3 % of the Ins+ cells, 940 counted cells, n=2 fish) (Figure 9G). At this stage, a large number of beta cells have recovered (about 30 to 50% of islet cells, Figure 9D) [2, 37] and glycemia was normalized (57 ± 9 mg/dl). In contrast, Insulin+ cells never harbor GFP labeling in non-treated fish (Figure 9E). Thus, by using the same approach of short-term tracing of nkx6.1:eGFP+ cells as in embryos, this finding strongly suggests that ductal nkx6.1:eGFP+ cells contribute to regenerated beta cells.

Next we assessed proliferation in *Tg(nkx6.1:eGFP); Tg(ins:NTR-mCherry)* in response to beta cell ablation. 3 days post treatment, *nkx6.1*:eGFP ductal cells showed increased proliferation as illustrated with PCNA (Figure 9H-I). This was observed not only within ductal structures as previously described ([2], and not shown) but also for CACs. These observations suggest that ductal cells with pancreatic progenitor properties activate proliferation prior differentiation into beta cells during regeneration.

Transcriptomic analysis of adult *nkx6.1*+ pancreatic ductal cells

To get a comprehensive characterization of pancreatic *nkx6.1*+ ductal cells in adult zebrafish, we determined their transcriptome landscape. Ductal GFP+ cells were isolated from dissected pancreas of adult *Tg(nkx6.1:eGFP)* fish (with ~95 % purity) and used in RNA-seq experiments. The expression of 15,888 genes could be detected in the ductal transcriptome (complete data available at http://www.ebi.ac.uk/ena/data/view/PRJEB10137),

in which many genes already known to be expressed in pancreatic ducts in either zebrafish or mammals were found at high expression level, such as *sox9b*, *hnf1ba*, *onecut1/hnf6*,*cftr*, *cdh17*, *ca2*, and *ctgfa* in addition to *nkx6.1* (Figure 10). We also detected expression of *fgfr4* and *sdc4*, recently proposed as novel ductal markers in the murine embryonic pancreas [38]. In contrast to these ductal genes, the acinar markers *ptf1a* and *rbpjl*, the pan-endocrine markers *pax6b* and *isl1*, and the lineage specific genes *mnx1* and *arx* were either not detected or detected at extremely low levels in the *nkx6.1:*eGFP+ ductal cells transcriptome (Figure 10), underscoring the accuracy of our FACS cell preparations. In contrast to mouse or human adults in which the embryonic pancreatic progenitor marker *Pdx1* is not expressed in the pancreatic ducts in normal condition, *nkx6.1:*eGFP+ duct cells of healthy zebrafish display a robust expression of *pdx1*. Comparison of the duct transcriptome with those of pancreatic acinar and endocrine cells (manuscript in preparation) highlighted 3,684 genes with preferential expression in duct cells. Among them, 293 duct-specific genes were identified with strong enrichment (≥16-fold) and low expression in the other pancreatic cells (Additional file 8: Supplemental Table 1), in which we find *sox9b*, *onecut1/hnf6*, *cdh17*, *ctgfa*, and *nkx6.1*,corroborating their status as duct-specific markers. Various components of the Notch signaling pathway could also be identified, namely *notch2*, and different *Hairy and enhancer of split*-related genes (*her6*, *her9*, *her15.1*), confirming that a subpopulation of *nkx6.1*+ cells (the CACs) experiences Notch activity. In addition to genes involved in the Notch signaling cascade, our analyses also identified novel duct-specific markers such as *id2a*, encoding for a HLH transcription factor, which we also detected co-expressed with *sox9b* by whole mount *in situ* hybridization in 3 dpf larvae (Additional file 9: Figure S8), and several components of the Wnt pathways such as the Wnt and SFRP ligands *sfrp5*, *sfrp3/frzb*, and *wnt7bb* (Additional file 8: Supplemental Table 1). At a lower expression level, we could also detect the Wnt receptor *fzd7a*, which was the only Wnt receptor significantly expressed in the adult pancreas (565 ± 106 normalized counts with 68-fold enrichment in the ducts). These observations suggest that Wnt signaling may play an important role in adult ducts.

Strikingly, the only endocrine transcription factor that displayed substantial expression (>1000 counts) and enrichment in the ductal transcriptome was the pro-endocrine gene *ascl1b* (Figure 10). As *ascl1b* specifically marks the endocrine precursors during pancreas development, these data support our observation that, within the *nkx6.1:*eGFP+ cell domain, some cells activate a pro-endocrine differentiation program in normal adult zebrafish.

Discussion

In this study, we determined during development the fate of two pancreatic cell populations marked by *nkx6.1* and *ascl1b* and found that *nkx6.1*+ cells are *bona fide* multipotent pancreatic progenitors while *ascl1b*+ cells represent committed endocrine precursors. We found also that *nkx6.1* is maintained in adult zebrafish in ducts and CAC/terminal end duct cells which we show still have the potential to give rise to endocrine cells in normal – non-diabetic – animals. The progenitor potency of adult *nkx6.1*+ cells is also reflected in their transcriptome through the expression of several pancreatic progenitor markers and by their capacity to generate new beta cells after beta cell ablation.

Although *ascl1b* marks the endocrine precursor cells, as opposed to *nkx6.1* which is the first multipotent pancreatic progenitor marker known to date, it is surprising to note that this transcription factor begins to be expressed in the prospective pancreatic region at 10 hpf [15], i.e. more than 1 hour before the appearance of *nkx6.1* (11.5 hpf) [18]. *Pdx1*, known in mouse to be also expressed in the multipotent pancreatic progenitors, appears even later (14 hpf, [6]). This brings the interesting concept that the first cells in the pancreatic anlagen acquire an endocrine identity before acquiring a pancreatic identity, suggesting that the mechanisms controlling pancreatic and endocrine identity are not necessary linked and can act in parallel. This situation seems to be restricted to the dorsal bud as, later, *nkx6.1* is first expressed during the formation of the ventral bud and *ascl1b* is then detected in endocrine committed cells. This peculiar situation could be related to the different lineage potential of the dorsal versus ventral bud cells. Indeed the dorsal bud gives rise exclusively to endocrine cells while the ventral bud is able to give rise to all pancreatic cell types [4, 39].

After a transient overlapping expression in the dorsal pancreatic anlagen, *nkx6.1* and *ascl1b* expressing domains segregate progressively. Cross-repressive interactions between lineage-determining transcription factors have been proposed as a molecular mechanism for establishing lineage allocation in several tissues [40-42]. We show that such a mechanism does not occur here as we could not observe any cross-repression between *nkx6.1* and *ascl1b* in the dorsal bud when analyzing both mutants. The segregation can instead be explained by an opposite effect of Notch signaling pathway on *nkx6.1* and *ascl1b* expression. By loss- and gain-of-function experiments, we definitely prove that *ascl1b* is repressed, while *nkx6.1* is maintained, by Notch signaling in both dorsal and ventral bud. The importance of Notch signaling in regulating *nkx6.1* expression has been also shown in mice where disruption of Notch signaling results in the loss of the “pro-trunk” determinant *Nkx6.1* and the acquisition of pro-acinar identity [43]. Direct binding of RBPJ-K to the *Nkx6.1* promoter supports a direct role of the Notch signaling in the expression of *Nkx6.1*. In contrast, the initiation of *nkx6.1* expression is independent of Notch signaling in both zebrafish pancreatic buds. This is in accordance with our findings that Nkx6.1+ cells progressively become Notch responsive, pancreatic Notch-responsive cells (PNCs) being found only in a subpopulation of

the Nkx6.1+ cells at the beginning of the formation of both dorsal and ventral buds. This could explain why the PNCs, found in a subdomain of the ventral bud at early stage, can differentiate only into ductal and endocrine cells, while *nkx6.1*-expressing cells give rise to all pancreatic cell types. As *nkx6.1* and *ptf1a* are initially co-expressed in the ventral bud primordium ([20] and our unpublished data), we can hypothesize that the *nkx6.1+/ptf1a+/*Notch ON cells give rise to the ductal and late endocrine cells while the *nkx6.1+/ptf1a+/*Notch OFF cells will give rise to the acinar cells. This model appears to contradict the data of Wang *et al.* [7] showing that the ventral bud primordium consists of two non-overlapping cell populations: a *ptf1*-expressing domain and a Notch-responsive progenitor core. It is possible that this discrepancy is due to the tools used to label the Notch-responsive cells: in our study, we used the *Tp1bglob:VenusPest* transgenic line allowing the detection of cells with current Notch activity, while Wang and collaborators used the *Tp1bglob:hgmb1-mCherry* line which could show a delay in mCherry detection.

In adult zebrafish, *nkx6.1* expression persists in the pancreas where it is specifically restricted to the ducts. This situation is different in mouse as *Nkx6.1* persists in beta cells but not in adult ducts. In zebrafish, it is *nkx6.2*, an *nkx6.1* homolog with functional equivalence [18, 44], which is expressed specifically in beta cells [18], suggesting that Nkx6 function in beta cell is fulfilled by Nkx6.2 in zebrafish. Persistence of *nkx6.1* expression in the zebrafish ducts is also associated with persistence of another pancreatic progenitor marker, *pdx1*, whose expression also restricts to beta cells in mammals. Combined with other hallmarks of embryonic pancreatic progenitors such as *sox9b*, *hnf1ba*, and Notch signaling components, the expression of *nkx6.1* and *pdx1* genes suggests that at least some ductal cells behave as pancreatic progenitors in adult zebrafish. Moreover, detection of the endocrine precursor marker *ascl1b* in the adult *nkx6.1:e*GFP+ ductal cell transcriptome is consistent with some ductal cells initiating an endocrine differentiation program and transiently expressing *ascl1b*, even in physiological conditions. The progenitor potential of ductal cells is fully revealed in the setting of beta cell regeneration where *nkx6.1:e*GFP+ cells show increased proliferation as well as the ability to differentiate into new beta cells. The adult pancreatic progenitors contributing to beta cell regeneration could be the CACs, as supported by our observation that they are able to replicate and to generate other ductal cells as well as endocrine beta cells. On the other hand, we cannot exclude the possibility that other ductal cells also contribute to regeneration based on *Tg(nkx6.1*:eGFP) which labels more broadly the ducts. Nevertheless, although the tool we used here to monitor lineage tracing presents some limitations (based on persistence of GFP protein to assess the short-term lineage tracing of *nkx6.1*-expressing cells), during the revision of our manuscript, a study by Delaspre *et al*. [37] established through CRE-based genetic labeling that Notch-responsive cells give rise to regenerated beta cells in adult zebrafish. Our data are in full accordance with their findings,

and support the conclusion that ductal cells, possibly CACs, possess regenerative capacity. To determine whether CACs only or other ductal cells contribute to beta cell regeneration will require other genetic lineage tracings with markers expressed only in ductular structures and not in CACs.

In contrast to mammals, the adult zebrafish has the remarkable capacity to rapidly and spontaneously regenerate its beta cells following their selective destruction [2]. Our findings showing that ductal cells, such as CACs, behave as pancreatic progenitors/stem cells in normal – non-diabetic – adult animals and during regeneration strongly suggest that they could also constitute a source of regenerated beta cells in diabetic mammalian models. In mouse, adult murine CACs display endocrine and exocrine progenitor potential *in vitro* with self-renewing ability [45], but evidences of their potential *in vivo* as progenitors of endocrine cells are missing. Indeed, CRE-based cell tracing of *Hes1*+ terminal duct cells/CACs in adult mice failed to show any islet progenitor capacity while these cells seemed to contribute to the ductal tree [46]. One explanation for this difference would be that while zebrafish CACs present pancreatic progenitor activity, mammalian CACs have retained a very limited capacity *in vivo* which could not be evidenced in the mouse model of beta cell regeneration used. Another explanation would be that CACs form a heterogeneous cell population. This latter hypothesis could be verified by the analysis of the expression of different ductal markers identified in our transcriptome that could help determine the existence of different ductal cell subpopulations.

A perspective of our work would be to thoroughly examine in zebrafish ductal cells in physiological conditions and during beta regeneration to identify mechanisms that could then be harnessed to promote beta cell regeneration in mammals. A first clue is provided by the fact that, *Nkx6.1* and *Pdx1* are normally not expressed in mammalian duct cells, in contrast to zebrafish. It is therefore tempting to hypothesize that inducing the expression of these two factors in the pancreatic ducts in adult mouse or human could enhance their progenitor potential. Consistent with this hypothesis, driving ectopic *Pdx1* expression is already harnessed for transdifferentiating different cells into beta cells *in vivo* (liver cells, pancreatic acinar cells, ...) [47-50] and for transdifferentiating pancreatic duct cells into beta cells *in vitro* [51]. Interestingly, the ability of *Pdx1* to reprogram liver cells into beta cells is substantially increased by the combined action of *Nkx6.1* [52], which potentiates induction of the early pancreatic master genes *Neurog3* and *Isl1*.

In the zebrafish larvae, two sources have been described for the regeneration of beta cells : progenitor cells in the developing ducts [35] and alpha cells [53]. From our data in adults, we cannot rule out the contribution by other cell types than ductal cells. Indeed, in addition to increased proliferation of ductal cells, some islets cells show also increased proliferation after beta cell destruction ([2] and our data not shown) suggesting the

involvement of other pancreatic, and possibly endocrine, cell types in regeneration. These possibilities remain to be validated in the adult zebrafish.

Our transcriptomic characterization of *nkx6.1*+ cells in normal, non regenerating, adult zebrafish identified many of the ductal markers known throughout species, showing that many of these genes and their expression are conserved between zebrafish and mammals as for example, different markers of Notch signaling [54-56], and *sdc4* and *fgfr4*. These latter two genes have been previously proposed as ductal markers in the mouse embryo [38]. Additional markers were also identified here, notably *id2a. Id2* has been shown to be expressed in ductal epithelial cells of IFNγNOD mice, a model of regenerating pancreas harboring hyperplasic ducts, and to be involved in their expansion [57]. We demonstrate here its expression in ducts in larvae and in healthy adult pancreas, which may correlate with a role in development and in ductal constitutive homeostasis. Our findings also reveal that, besides the Notch pathway, ductal cells specifically express various components of Wnt signaling pathways. The expression of the *fzd7a* receptor, of two secreted Wnt antagonists, *sfrp5* and *frzb/sfrp3*, and of the agonist *wnt7bb* suggests a complex control of the activity of the Wnt pathway(s) in adult pancreatic ducts. Whether and how these different factors orchestrate pancreatic duct development, homeostasis and function remains to be determined. Numerous cross-talks between the Notch and the Wnt/beta-catenin pathways occur during development, tissue homeostasis and disease, notably by regulating the balance of stem cells and differentiated cells (reviewed in [58]). During pancreas development, beta-catenin controls the patterning of multipotent versus bipotent embryonic pancreatic progenitors in mouse, in part, by inhibiting Notch signaling [59]. Our findings raise the question whether similar interactions shape fate decision of progenitors/stem cells in the adult pancreas.

Conclusions

We have developed transgenic tools enabling the characterization of *nkx6.1*+ and *ascl1b*+ progenitor cell populations and showed that, in the zebrafish embryo, *nkx6.1*+ cells are multipotent pancreatic progenitors, while *ascl1b*+ cells represent committed endocrine precursors. In adult zebrafish, *nkx6.1* expression persists exclusively in the ductal tree, notably in CACs. Transcriptomic profiling of adult *nkx6.1*+ ductal cells reveals hallmarks of embryonic pancreatic progenitors, as well as identify novel ductal markers. Our data also strongly suggest that adult zebrafish ductal cells, possibly CACs, possess regenerative capacity. Further characterization of ductal cells in this animal model should bring new insight into regeneration in mammals and open up new perspectives for anti-diabetic therapies.

Methods

Zebrafish maintenance, mutant and transgenic lines and LY411575 treatment:

Zebrafish (*Danio rerio*) were raised and cared for according to standard protocols [60]. All animal work has been conducted according to national guidelines and all animal experiments described herein were approved by the ethical committee of the University of Liège (protocol numbers 371, 1285 and 1662). Wild-type embryos from the AB strain were used and staged according to Kimmel [61]. Homozygous mind bomb mutants were obtained by mating heterozygous fish for the (mib^{ta52b}) allele [62]. The following transgenic lines were used : *Tg(hsp70l:Gal4)1.5*^{kca4} abbreviated *Tg(hsp:Gal4)* and *Tg(UAS:myc-Notch1a-intra)*^{kca3} abbreviated *Tg(UAS:NICD)* [33], *Tg(Tp1bglob:eGFP)*^{um14} abbreviated *Tg(Tp1:eGFP)* [12], *Tg(TP1bglob:VenusPest)*^{S940}abbreviated *Tg(TP1:VenusPest)* [16], *Tg(Tp1bglob:H2BmCherry)*^{S939} abbreviated *Tg(Tp1:H2BmCherry)* [16], Tg(*ubi:loxP-EGFP-loxP-mCherry)* abbreviated *ubi:Switch* [28], *Tg(ubi:loxP-AmCyan-loxP-ZsYellow)* abbreviated *ubi:CSY* [27]; *Tg(ins:NTR-mCherry)* [1] and *Tg(nkx6.1:eGFP); Tg(ins:NTR-mCherry)*.

The LY411575 treatment was performed by incubating the embryos during the indicated period with a 10 µm LY411575 solution (Medchemexpress), replaced every day.

Generation of BAC transgenic lines:

The PCR primers used to generate the constructs are listed in Additional file 10, Supplemental Table 2. The *BAC:nkx6.1* (Imagenes, DKEY-173K2) DNA was introduced by electroporation into SW102 *E. coli* (derived from DY380) [63]. These bacteria contain the lambda prophage recombineering system and a galactose operon where the galactokinase gene (*galK*) has been deleted. The e*GFP* gene was inserted into the exon 1 *of nkx6.1*, replacing the beginning of the *nkx6.1* open reading frame (aa 1 to 149) using a two-step positive and negative *galk* selection [25, 63, 64]. During the first step, the cassette containing the *galk* gene was amplified by PCR with the primers pair O180F and O253R, containing at the 5'end 50 bases identical to *nkx6.1* sequence to allow homologous recombination and electroporated into the bacteria SW102 containing the *BAC:nkx6.1*. Only recombinant bacteria are able to grow on minimal medium containing galactose as carbon source. During the second step, the *galK* gene was replaced by the e*GFP* gene. The *eGFP* cassette was amplified by PCR with the primers O186F and O256R containing at the 5'-end the same 50 bases identical to *nkx6.1* sequence to allow homologous recombination and the *eGFP* sequences to anneal to the *eGFP* cassette. After electroporation, the bacteria are plated on minimal medium containing two-deoxy-D-galactose (DOG), a galactose analogue that after

phosphorylation by GalK, becomes toxic. Only bacteria which have lost the *galk* gene survived on DOG-containing medium. To facilitate the insertion of the BAC in the genome of zebrafish, the *iTol2* cassette was also inserted into the backbone of *the BAC:nkx6.1-eGFP* [24, 25, 64]. The *iTol2* cassette was amplified by PCR with the primers pair O215F and O216R. The final construct *(BAC:nkx6.1-eGFP)* was purified with Nucleobond® BAC100 (MACHEREY-NAGEL) and injected into the cytoplasm of one-cell stage zebrafish embryos together with the mRNA for the transposase. The embryos and larvae were screened for GFP expression and the fluorescent injected fish were raised to adulthood and the offspring was screened for fluorescence. The transgenic line obtained was abbreviated to *Tg(nkx6.1:eGFP)* in the article.

To generate the *(ascl1b:eGFP-2A-creER^{T2})*transgenic line, we used *BAC:ascl1b* (Imagenes, DKEY-265N18) spanning from 61 kb upstream and 89 kb downstream of the *ascl1b* gene. The *GFP-2A-creER^{T2}* cassette was inserted into the exon 1 of *ascl1b*, replacing the beginning of the *ascl1b* open reading frame (aa 1 to 163) using the same two-step positive and negative *galk* selection as described above. For the first step, the cassette containing the *galk* gene was obtained by PCR using the primers O275F and O276R and for the second step, the *GFP-2A-creER^{T2}*cassette was amplified using the primers O277F and O278R.

4OHT treatment for creER^{T2} induction:

4-Hydroxytamoxifen (4OHT, Sigma H7904) was dissolved in DMSO as a stock solution of 10 mM and kept in single-use aliquots in the dark at -70°C. A working concentration of 10 µM 4OHT was demonstrated to optimally lead to Cre-mediated recombination without causing deleterious development defects. Embryos were treated 5 times from 11 to 15 hpf in E3 containing 10 µM 4OHT and kept in the dark at 28°C. After the treatments, the embryos were washed in fresh E3 and fixed at 48hpf or 72hpf.

CRISPR/cas9 genome mutagenesis

The *nkx6.1* and *ascl1b* mutant lines were generated by CRISPR/Cas9 technology essentially as described previously [31, 65]. The targeted sites were selected using the ZiFiT software package (http://zifit.partners.org/ZiFiT/) in the first exon of *nkx6.1* (CCAAACCCCTGACAGAGCTTC) before the homeodomain coding region and in the first exon of *ascl1b* (GGAGACGCTGCGCTCCGCCGTGG) corresponding to the helix-loop-helix coding domain. The selected oligonucleotides were inserted in the plasmid DR274 (Addgene) and the gRNA were synthesized by *in vitro* transcription using T7 RNA polymerase. Fertilized zebrafish eggs were injected with about 1nl of solution containing 50ng of gRNA and 300ng of nls-zCas9-nls mRNA obtained by transcription of the plasmid

pT3TS-nCas9n (Addgene). Efficiency of mutagenesis was verified by genotyping using Heteroduplex Migration Assays [66] after amplification of targeted genomic sequences. Injected embryos were raised until adulthood and cross with wild type fish to generate heterozygote mutant F1 fish. Fish harboring frame-shift mutations were kept and used to raise F2 mutant lines i.e the *ascl1b*$^{ulg\text{-}M2C}$ and *nkx6.1*$^{ulg\text{-}M5}$ lines carrying respectively 11 and 7 nucleotide deletions.

Whole mount *in situ* hybridization, whole mount immunohistochemistry and immunohistochemistry on paraffin sections.

Double Fluorescent and visible whole-mount *in situ* hybridizations were performed as previously described [67, 68] with the following probes : *ascl1b* [15, 69], *nkx6.1* [18, 70], *somatostatin 2 (sst2)* [71] and *try* [6].

Immunohistochemistry (IHC) on whole mount embryos has been performed as described [15]. For IHC on paraffin section with adult tissues, adult fish between 6 and 9 months old were fixed in 4% PFA overnight at 4° after euthanasia and opening of the abdominal skin. The digestive tract was then dissected and embedded in paraffin following standard procedures. 5 µm sections were collected through the head of the pancreas at the level of the main pancreatic islet. Immunodetections were performed after standard antigen retrieval.

The antibodies used were : polyclonal rabbit anti-mCherry/dsRed (Living Colors DsRed Polyclonal Antibody, Clontech) 1:500, polyclonal rabbit anti-ZsYellow (The living colors anti-RCFP polyclonal pan from Clontech) 1:300, chicken anti-GFP (Aves lab) 1:1000, mouse monoclonal anti-Nkx6.1 (clone F55A10) 1:20, mouse monoclonal anti-Isl1 (Hybridoma bank) 1:50; guinea pig anti-Insulin (Dako) 1:500, mouse anti-Glucagon (Sigma) 1:300, polyclonal rabbit anti-Somatostatin (MP Biomedicals) 1:300, mouse anti-PCNA (Sigma) 1:1000, mouse 2F11 mAb (Abcam) 1:1000, Alexa Fluor secondary antibodies (Invitrogen). Venus was detected with anti-GFP. DAPI was used as nuclear staining.

Images were acquired with a Leica SP2 or SP5 confocal microscope and processed with Imaris 7.2.3 and Photoshop CS5. For the counting of Tp1:H2BmCherry+ cells expressing Insulin, the total pancreatic mCherry+/Venus- cells and the mCherry+/Ins+ was calculated in 6 sections every 15 µm in 4 fish.

EdU injection and detection in adult zebrafish

A 12.5 mM EdU solution in DPBS containing 0.25% DMSO was injected intraperitoneally in 6 to 9 month-old fish at 100 µg/g body weight after anesthesia in tricaïne methane sulfonate. Fish were then sacrificed and fixed in 4% PFA. EdU (Click-iT® Labeling Technologies, Life Technologies) incorporation was detected on paraffin sections with Alexa Fluor555 before proceeding to immunohistochemistry detection.

For the counting of EdU+ cells, the total pancreatic Venus+ CAC and Venus+/EdU+ cells was calculated in 3 to 6 sections every 15 µm in 4 fish.

Induction of beta cell ablation in adult zebrafish

Adult *Tg(nkx6.1:eGFP); Tg(ins:NTR-mCherry)* zebrafish between 6 and 9 months old were treated in fish water containing 10 mM metronidazole (MTZ) (3-4 fish/500 ml, Sigma 3761) for 20 hours at 28°C. Then the water was replaced twice before re-integration into the system.

Fish were anesthetized with tricaïne and their glycemia was measured using the Accu-Chek Aviva glucometer system (Roche Diagnostics) with blood collected at the level of the tail. To minimize variations, the fish were fasted for 24 hours before measurement. After decapitation, the whole fish were fixed in 4% PFA overnight at 4°C. The digestive tract was then dissected prior to paraffin embedding.

FACS purification of ductal cells

The pancreas of 3 to 5 *Tg(nkx6.1:eGFP*) adult fish (6-9 month-old) were dissected and collected in HBSS with Calcium. Dissociation was performed in HBSS with Ca2+/Mg2+ supplemented with 1 mg/ml collagenase IV (Life Technologies 17104-019) and collagenase P (Roche 1121386501) and 1.5 mg/ml dispase II (Life Technologies 17105-041) for 20 min at 30°. After several washes in HBSS w/o Ca2+/Mg2+, single cell suspension was obtained by Tryple Select 1x incubation during 10 min. Dissociation was stopped by HBSS w/o Ca2+/Mg2+ containing 1% BSA and 2 mM EDTA. GFP+ cells were isolated on FACS Aria II under Purity Mode and the purity of the sorted cells was confirmed on a small fraction under epifluorescence microscope (~95 %). Cells were immediately lyzed in 3.5 µl Reaction Buffer (SMARTer Ultra Low RNA kit for Illumina sequencing, Clontech) and stored at -80°C. Three independent replicates were generated from 6 to 9 months old fish.

cDNA synthesis and library preparation

cDNA synthesis was performed using the SMARTer Ultra Low RNA kit for Illumina sequencing (Clontech) according manufacturer's recommendations. 3.000 to 5.000 sorted GFP+ cells were directly lyzed in 3.5 µl Reaction Buffer and immediately frozen at -80°C. cDNAs were synthesized, purified with Ampure XP beads and then amplified with 13 PCR cycles with Advantage 2 Polymerase Mix (50×, Clontech). The PCR products were purified on SPRI AMPure XP beads (Beckman Coulter), and size distribution was checked on a High-Sensitivity DNA chip (Agilent Bioanalyzer). cDNA libraries were prepared with TruSeq Nano DNA kit or Nextera XT DNA (Illumina). For TruSeq Nano libraries, 20 to 30 ng cDNA were sheared by sonication (parameters adjusted to obtain fragments from 350 to 450 bp). For Nextera libraries, 1 ng was fragmented by tagmentation. Then cDNA libraries were prepared according manufacturer's recommendations. Samples were sequenced on Illumina HiSeq 2000 at on average 72.3 millions 100 bp paired-end reads. RNA-seq data have been deposited in the European Nucleotide Archive from EMBL-EBI at http://www.ebi.ac.uk/ena/data/view/PRJEB10137.

Data analysis of the duct transcriptome

Before mapping, the first 30 bases of each read were trimmed in order to remove the adapters incorporated by the cDNA synthesis process. Trimmed reads were mapped to the zebrafish genome (Zv9, Ensembl genes version 75, ensembl.org) using the Tophat v.2.0.9 software [72]. The mapping summary for the three replicates is: Duct 1: 40,336,250 total number of reads, 79.9% mapped; Duct 2: 86,308,531 total number of reads, 82.5% mapped; Duct 3: 91,980,011 total number of reads, 67.6% mapped.

HT-Seq count was used to estimate the expression level by counting how many reads align to each gene of the annotation (gene set, Ensembl.org) [73]. The expression of 15,888 genes was detected with at least 1 read in all three replicates.

In order to describe the set of genes enriched or preferentially expressed in ductal tissue, the ductal transcriptome was compared with acinar and endocrine transcriptomes prepared following the same methodology (composed of alpha, beta, delta cells, not shown here, manuscript in preparation). The R package EBSeq was used to call differential expressed genes [74]. Ductal genes were identified based on their posterior probability (adjusted by FDR) of being differentially expressed from the other two cell types. 3,684 genes were found preferentially expressed in the duct transcriptome. Stricter thresholds were applied to identify genes with highly specific ductal expression (see Results).

Abbreviations:

4OH: 4-hydroxytamoxifen; ASCL: Achaete-Scute Like; ARP: Atonal Related Protein; BAC: bacterial artificial Chromosome; bHLH: basic helix-loop-helix; CAC: centroacinar/terminal duct cells; creER^{T2}: 4OHT inducible Cre-recombinase; dpf: days post fertilization; dpt: days post treatment; EdU: 5-ethynyl-2'-deoxyuridine; eGFP: enhanced green protein; EPD: extra-pancreatic ducts; FACS: Fluorescence-Activated Cell Sorting; Gcg: Glucagon; hpf: hours post fertilization; IHC: immunohistochemistry; Ins: Insulin; IPD : intra-pancreatic ducts; MTZ: metronidazole; NICD: Notch intracellular domain; PNCs: pancreatic Notch-responsive cells; Rec Marker: Recombinant marker; Sst: Somatostatin; VenusPEST: Venus fluorescent protein; WISH: Whole-mount in situ hybridization; wt: wild type.

Authors' contributions

APG and DB participated in the design of the study, generated the data and participated in their interpretation and in the drafting of the manuscript. ETS carried out the RNA-seq analyzes. LCF initiated the study on *ascl1b* (design and experiments). VVB participated in the generation of experimental data. BP participated in the design of the study and in data interpretation and helped draft the manuscript. MLV and IM conceived the study, participated in the interpretation of the data and wrote the manuscript. All authors read and approved the final manuscript.

Acknowledgments :

We are grateful to Christian Mosiman for the tamoxifen treatment advices and Marielle Lebrun and Alain Vanderplasschen for the galk recombineering advices. We thank Koichi Kawakami for the itol2 cassette [25]. We are very grateful to Didier Stainier and Nicolay Ninov for the transgenic lines *Tg(Tp1:VenusPest) and Tg(Tp1:H2BmCherry)* [16], Francesco Argenton for the Tg(Tp1glob:eGFP) [12], Carole Wilson (UCL fish facility, UK) for the *Tg(ubi:Switch)* [28], Geoffrey Burns for *Tg(ubi:loxP-AmCyan-loxP-ZsYellow)*, Jean-Claude TWIZERE for the *Tg(hsp70:Gal4)* and *Tg(UAS:myc-notch1a-intra)* [33]. We thank the following technical platforms: GIGA-Zebrafish (M. Winandy and H. Pendeville), GIGA-Cell Imaging and Flow Cytometry platform (S. Ormenese and S. Raafat), GIGA-Genotranscriptomic (B. Hennuy, W. Coppieters and L. Karim) and GIGA-Immunohistochemistry (C. Humblet and E. Dortu).

A.G and D.B were supported by the FRIA and the Léon Fredericq fund, E.T by the WBI and the Léon Fredericq fund, V.V.B by the Belgian State's “Interuniversity Attraction Poles” Program (SSTC, PAI). B.P, I.M. and M.L.V. are "Chercheur qualifié" FNRS. This work was funded by the FNRS-FRS, the Belgian State's “Interuniversity Attraction Poles” Program (SSTC, PAI) and the “Fonds Speciaux” from the ULg.

Competing interests :

The authors declare that they have no competing interests.

References:

1. Pisharath H, Rhee JM, Swanson MA, Leach SD, Parsons MJ: **Targeted ablation of beta cells in the embryonic zebrafish pancreas using E. coli nitroreductase**. *Mech Dev* 2007, **124**(3):218-229.
2. Moss JB, Koustubhan P, Greenman M, Parsons MJ, Walter I, Moss LG: **Regeneration of the pancreas in adult zebrafish**. *Diabetes* 2009, **58**(8):1844-1851.
3. Curado S, Anderson RM, Jungblut B, Mumm J, Schroeter E, Stainier DY: **Conditional targeted cell ablation in zebrafish: a new tool for regeneration studies**. *Dev Dyn* 2007, **236**(4):1025-1035.
4. Field HA, Dong PD, Beis D, Stainier DY: **Formation of the digestive system in zebrafish. II. Pancreas morphogenesis**. *Developmental biology* 2003, **261**(1):197-208.
5. Kumar M, Melton D: **Pancreas specification: a budding question**. *Current opinion in genetics & development* 2003, **13**(4):401-407.
6. Biemar F, Argenton F, Schmidtke R, Epperlein S, Peers B, Driever W: **Pancreas development in zebrafish: early dispersed appearance of endocrine hormone expressing cells and their convergence to form the definitive islet**. *Developmental biology* 2001, **230**(2):189-203.
7. Wang Y, Rovira M, Yusuff S, Parsons MJ: **Genetic inducible fate mapping in larval zebrafish reveals origins of adult insulin-producing beta-cells**. *Development* 2011, **138**(4):609-617.
8. Hesselson D, Anderson RM, Beinat M, Stainier DY: **Distinct populations of quiescent and proliferative pancreatic beta-cells identified by HOTcre mediated labeling**. *Proceedings of the National Academy of Sciences of the United States of America* 2009, **106**(35):14896-14901.
9. Kimmel RA, Onder L, Wilfinger A, Ellertsdottir E, Meyer D: **Requirement for Pdx1 in specification of latent endocrine progenitors in zebrafish**. *BMC Biol* 2011, **9**:75.
10. Chung WS, Andersson O, Row R, Kimelman D, Stainier DY: **Suppression of Alk8-mediated Bmp signaling cell-autonomously induces pancreatic beta-cells in zebrafish**. *Proceedings of the National Academy of Sciences of the United States of America* 2010, **107**(3):1142-1147.
11. Dong PD, Munson CA, Norton W, Crosnier C, Pan X, Gong Z, Neumann CJ, Stainier DY: **Fgf10 regulates hepatopancreatic ductal system patterning and differentiation**. *Nat Genet* 2007, **39**(3):397-402.

12. Parsons MJ, Pisharath H, Yusuff S, Moore JC, Siekmann AF, Lawson N, Leach SD: **Notch-responsive cells initiate the secondary transition in larval zebrafish pancreas**. *Mech Dev* 2009, **126**(10):898-912.
13. Afelik S, Jensen J: **Notch signaling in the pancreas: patterning and cell fate specification**. *Wiley Interdiscip Rev Dev Biol* 2013, **2**(4):531-544.
14. Apelqvist A, Li H, Sommer L, Beatus P, Anderson DJ, Honjo T, Hrabe de Angelis M, Lendahl U, Edlund H: **Notch signalling controls pancreatic cell differentiation**. *Nature* 1999, **400**(6747):877-881.
15. Flasse LC, Pirson JL, Stern DG, Von Berg V, Manfroid I, Peers B, Voz ML: **Ascl1b and Neurod1, instead of Neurog3, control pancreatic endocrine cell fate in zebrafish**. *BMC Biol* 2013, **11**:78.
16. Ninov N, Borius M, Stainier DY: **Different levels of Notch signaling regulate quiescence, renewal and differentiation in pancreatic endocrine progenitors**. *Development* 2012, **139**(9):1557-1567.
17. Zhou Q, Law AC, Rajagopal J, Anderson WJ, Gray PA, Melton DA: **A multipotent progenitor domain guides pancreatic organogenesis**. *Dev Cell* 2007, **13**(1):103-114.
18. Binot AC, Manfroid I, Flasse L, Winandy M, Motte P, Martial JA, Peers B, Voz ML: **Nkx6.1 and nkx6.2 regulate alpha- and beta-cell formation in zebrafish by acting on pancreatic endocrine progenitor cells**. *Dev Biol* 2010, **340**(2):397-407.
19. Schaffer AE, Freude KK, Nelson SB, Sander M: **Nkx6 transcription factors and Ptf1a function as antagonistic lineage determinants in multipotent pancreatic progenitors**. *Dev Cell* 2010, **18**(6):1022-1029.
20. Hesselson D, Anderson RM, Stainier DY: **Suppression of Ptf1a activity induces acinar-to-endocrine conversion**. *Current biology : CB* 2011, **21**(8):712-717.
21. Dong PD, Provost E, Leach SD, Stainier DY: **Graded levels of Ptf1a differentially regulate endocrine and exocrine fates in the developing pancreas**. *Genes Dev* 2008, **22**(11):1445-1450.
22. Manfroid I, Ghaye A, Naye F, Detry N, Palm S, Pan L, Ma TP, Huang W, Rovira M, Martial JA *et al*: **Zebrafish sox9b is crucial for hepatopancreatic duct development and pancreatic endocrine cell regeneration**. *Dev Biol* 2012, **366**(2):268-278.
23. Sander M, Sussel L, Conners J, Scheel D, Kalamaras J, Dela Cruz F, Schwitzgebel V, Hayes-Jordan A, German M: **Homeobox gene Nkx6.1 lies downstream of Nkx2.2 in the major pathway of beta-cell formation in the pancreas**. *Development* 2000, **127**(24):5533-5540.
24. Suster ML, Sumiyama K, Kawakami K: **Transposon-mediated BAC transgenesis in zebrafish and mice**. *BMC Genomics* 2009, **10**:477.
25. Suster ML, Abe G, Schouw A, Kawakami K: **Transposon-mediated BAC transgenesis in zebrafish**. *Nat Protoc* 2011, **6**(12):1998-2021.
26. Corish P, Tyler-Smith C: **Attenuation of green fluorescent protein half-life in mammalian cells**. *Protein engineering* 1999, **12**(12):1035-1040.
27. Zhou Y, Cashman TJ, Nevis KR, Obregon P, Carney SA, Liu Y, Gu A, Mosimann C, Sondalle S, Peterson RE *et al*: **Latent TGF-beta binding protein 3 identifies a second heart field in zebrafish**. *Nature* 2011, **474**(7353):645-648.
28. Mosimann C, Kaufman CK, Li P, Pugach EK, Tamplin OJ, Zon LI: **Ubiquitous transgene expression and Cre-based recombination driven by the ubiquitin promoter in zebrafish**. *Development* 2011, **138**(1):169-177.
29. Chung WS, Shin CH, Stainier DY: **Bmp2 signaling regulates the hepatic versus pancreatic fate decision**. *Dev Cell* 2008, **15**(5):738-748.
30. Chung WS, Stainier DY: **Intra-endodermal interactions are required for pancreatic beta cell induction**. *Dev Cell* 2008, **14**(4):582-593.
31. Hwang WY, Fu Y, Reyon D, Maeder ML, Tsai SQ, Sander JD, Peterson RT, Yeh JR, Joung JK: **Efficient genome editing in zebrafish using a CRISPR-Cas system**. *Nat Biotechnol* 2013, **31**(3):227-229.

32. Itoh M, Kim CH, Palardy G, Oda T, Jiang YJ, Maust D, Yeo SY, Lorick K, Wright GJ, Ariza-McNaughton L *et al*: **Mind bomb is a ubiquitin ligase that is essential for efficient activation of Notch signaling by Delta**. *Dev Cell* 2003, **4**(1):67-82.
33. Scheer N, Groth A, Hans S, Campos-Ortega JA: **An instructive function for Notch in promoting gliogenesis in the zebrafish retina**. *Development* 2001, **128**(7):1099-1107.
34. Lorent K, Moore JC, Siekmann AF, Lawson N, Pack M: **Reiterative use of the notch signal during zebrafish intrahepatic biliary development**. *Dev Dyn* 2010, **239**(3):855-864.
35. Ninov N, Hesselson D, Gut P, Zhou A, Fidelin K, Stainier DY: **Metabolic regulation of cellular plasticity in the pancreas**. *Current biology : CB* 2013, **23**(13):1242-1250.
36. Matsuda H, Parsons MJ, Leach SD: **Aldh1-expressing endocrine progenitor cells regulate secondary islet formation in larval zebrafish pancreas**. *PLoS One* 2013, **8**(9):e74350.
37. Delaspre F, Beer RL, Rovira M, Huang W, Wang G, Gee S, Vitery MD, Wheelan SJ, Parsons MJ: **Centroacinar cells are progenitors that contribute to endocrine pancreas regeneration**. *Diabetes* 2015.
38. Shih HP, Kopp JL, Sandhu M, Dubois CL, Seymour PA, Grapin-Botton A, Sander M: **A Notch-dependent molecular circuitry initiates pancreatic endocrine and ductal cell differentiation**. *Development* 2012, **139**(14):2488-2499.
39. Zecchin E, Mavropoulos A, Devos N, Filippi A, Tiso N, Meyer D, Peers B, Bortolussi M, Argenton F: **Evolutionary conserved role of ptf1a in the specification of exocrine pancreatic fates**. *Developmental biology* 2004, **268**(1):174-184.
40. Briscoe J, Pierani A, Jessell TM, Ericson J: **A homeodomain protein code specifies progenitor cell identity and neuronal fate in the ventral neural tube**. *Cell* 2000, **101**(4):435-445.
41. Olguin HC, Yang Z, Tapscott SJ, Olwin BB: **Reciprocal inhibition between Pax7 and muscle regulatory factors modulates myogenic cell fate determination**. *The Journal of cell biology* 2007, **177**(5):769-779.
42. Laslo P, Spooner CJ, Warmflash A, Lancki DW, Lee HJ, Sciammas R, Gantner BN, Dinner AR, Singh H: **Multilineage transcriptional priming and determination of alternate hematopoietic cell fates**. *Cell* 2006, **126**(4):755-766.
43. Afelik S, Qu X, Hasrouni E, Bukys MA, Deering T, Nieuwoudt S, Rogers W, Macdonald RJ, Jensen J: **Notch-mediated patterning and cell fate allocation of pancreatic progenitor cells**. *Development* 2012, **139**(10):1744-1753.
44. Nelson SB, Schaffer AE, Sander M: **The transcription factors Nkx6.1 and Nkx6.2 possess equivalent activities in promoting beta-cell fate specification in Pdx1+ pancreatic progenitor cells**. *Development* 2007, **134**(13):2491-2500.
45. Rovira M, Scott SG, Liss AS, Jensen J, Thayer SP, Leach SD: **Isolation and characterization of centroacinar/terminal ductal progenitor cells in adult mouse pancreas**. *Proceedings of the National Academy of Sciences of the United States of America* 2010, **107**(1):75-80.
46. Kopinke D, Brailsford M, Shea JE, Leavitt R, Scaife CL, Murtaugh LC: **Lineage tracing reveals the dynamic contribution of Hes1+ cells to the developing and adult pancreas**. *Development* 2011, **138**(3):431-441.
47. Zhou Q, Brown J, Kanarek A, Rajagopal J, Melton DA: **In vivo reprogramming of adult pancreatic exocrine cells to beta-cells**. *Nature* 2008, **455**(7213):627-632.
48. Ferber S, Halkin A, Cohen H, Ber I, Einav Y, Goldberg I, Barshack I, Seijffers R, Kopolovic J, Kaiser N *et al*: **Pancreatic and duodenal homeobox gene 1 induces expression of insulin genes in liver and ameliorates streptozotocin-induced hyperglycemia**. *Nat Med* 2000, **6**(5):568-572.
49. Shternhall-Ron K, Quintana FJ, Perl S, Meivar-Levy I, Barshack I, Cohen IR, Ferber S: **Ectopic PDX-1 expression in liver ameliorates type 1 diabetes**. *J Autoimmun* 2007, **28**(2-3):134-142.
50. Ber I, Shternhall K, Perl S, Ohanuna Z, Goldberg I, Barshack I, Benvenisti-Zarum L, Meivar-Levy I, Ferber S: **Functional, persistent, and extended liver to pancreas transdifferentiation**. *J Biol Chem* 2003, **278**(34):31950-31957.

51. Miyashita K, Miyatsuka T, Matsuoka TA, Sasaki S, Takebe S, Yasuda T, Watada H, Kaneto H, Shimomura I: **Sequential introduction and dosage balance of defined transcription factors affect reprogramming efficiency from pancreatic duct cells into insulin-producing cells**. *Biochem Biophys Res Commun* 2014, **444**(4):514-519.
52. Gefen-Halevi S, Rachmut IH, Molakandov K, Berneman D, Mor E, Meivar-Levy I, Ferber S: **NKX6.1 promotes PDX-1-induced liver to pancreatic beta-cells reprogramming**. *Cell Reprogram* 2010, **12**(6):655-664.
53. Ye L, Robertson MA, Hesselson D, Stainier DY, Anderson RM: **Glucagon is essential for alpha cell transdifferentiation and beta cell neogenesis**. *Development* 2015, **142**(8):1407-1417.
54. Miyamoto Y, Maitra A, Ghosh B, Zechner U, Argani P, Iacobuzio-Donahue CA, Sriuranpong V, Iso T, Meszoely IM, Wolfe MS *et al*: **Notch mediates TGF alpha-induced changes in epithelial differentiation during pancreatic tumorigenesis**. *Cancer Cell* 2003, **3**(6):565-576.
55. Strobel O: **In vivo lineage tracing defines the role of acinar-to-ductal transdifferentiation in inflammatory ductal metaplasia**. *Gastroenterology* 2007, **133**:1999-2009.
56. Stanger BZ, Stiles B, Lauwers GY, Bardeesy N, Mendoza M, Wang Y, Greenwood A, Cheng KH, McLaughlin M, Brown D *et al*: **Pten constrains centroacinar cell expansion and malignant transformation in the pancreas**. *Cancer Cell* 2005, **8**(3):185-195.
57. Hua H, Zhang YQ, Dabernat S, Kritzik M, Dietz D, Sterling L, Sarvetnick N: **BMP4 regulates pancreatic progenitor cell expansion through Id2**. *J Biol Chem* 2006, **281**(19):13574-13580.
58. Collu GM, Hidalgo-Sastre A, Brennan K: **Wnt-Notch signalling crosstalk in development and disease**. *Cell Mol Life Sci* 2014, **71**(18):3553-3567.
59. Baumgartner BK, Cash G, Hansen H, Ostler S, Murtaugh LC: **Distinct requirements for beta-catenin in pancreatic epithelial growth and patterning**. *Developmental biology* 2014, **391**(1):89-98.
60. Westerfield M: **The zebrafish book : a guide for the laboratory use of zebrafish (Danio rerio)**, Ed. 3. edn. [Eugene, OR]: M. Westerfield; 1995.
61. Kimmel CB, Ballard WW, Kimmel SR, Ullmann B, Schilling TF: **Stages of embryonic development of the zebrafish**. *Dev Dyn* 1995, **203**(3):253-310.
62. Haddon C, Jiang YJ, Smithers L, Lewis J: **Delta-Notch signalling and the patterning of sensory cell differentiation in the zebrafish ear: evidence from the mind bomb mutant**. *Development* 1998, **125**(23):4637-4644.
63. Warming S, Costantino N, Court DL, Jenkins NA, Copeland NG: **Simple and highly efficient BAC recombineering using galK selection**. *Nucleic acids research* 2005, **33**(4):e36.
64. Bussmann J, Schulte-Merker S: **Rapid BAC selection for tol2-mediated transgenesis in zebrafish**. *Development* 2011, **138**(19):4327-4332.
65. Jao LE, Wente SR, Chen W: **Efficient multiplex biallelic zebrafish genome editing using a CRISPR nuclease system**. *Proceedings of the National Academy of Sciences of the United States of America* 2013, **110**(34):13904-13909.
66. Ota S, Hisano Y, Muraki M, Hoshijima K, Dahlem TJ, Grunwald DJ, Okada Y, Kawahara A: **Efficient identification of TALEN-mediated genome modifications using heteroduplex mobility assays**. *Genes Cells* 2013, **18**(6):450-458.
67. Mavropoulos A, Devos N, Biemar F, Zecchin E, Argenton F, Edlund H, Motte P, Martial JA, Peers B: **sox4b is a key player of pancreatic alpha cell differentiation in zebrafish**. *Developmental biology* 2005, **285**(1):211-223.
68. Hauptmann G, Gerster T: **Two-color whole-mount in situ hybridization to vertebrate and Drosophila embryos**. *Trends Genet* 1994, **10**(8):266.
69. Allende ML, Weinberg ES: **The expression pattern of two zebrafish achaete-scute homolog (ash) genes is altered in the embryonic brain of the cyclops mutant**. *Developmental biology* 1994, **166**(2):509-530.
70. Cheesman SE, Layden MJ, Von Ohlen T, Doe CQ, Eisen JS: **Zebrafish and fly Nkx6 proteins have similar CNS expression patterns and regulate motoneuron formation**. *Development* 2004, **131**(21):5221-5232.

71. Argenton F, Zecchin E, Bortolussi M: **Early appearance of pancreatic hormone-expressing cells in the zebrafish embryo**. *Mechanisms of development* 1999, **87**(1-2):217-221.
72. Trapnell C, Roberts A, Goff L, Pertea G, Kim D, Kelley DR, Pimentel H, Salzberg SL, Rinn JL, Pachter L: **Differential gene and transcript expression analysis of RNA-seq experiments with TopHat and Cufflinks**. *Nat Protoc* 2012, **7**(3):562-578.
73. Anders S, Pyl PT, Huber W: **HTSeq-a Python framework to work with high-throughput sequencing data**. *Bioinformatics* 2014.
74. Leng N, Dawson JA, Thomson JA, Ruotti V, Rissman AI, Smits BM, Haag JD, Gould MN, Stewart RM, Kendziorski C: **EBSeq: an empirical Bayes hierarchical model for inference in RNA-seq experiments**. *Bioinformatics* 2013, **29**(8):1035-1043.
75. Nikolaou N, Watanabe-Asaka T, Gerety S, Distel M, Koster RW, Wilkinson DG: **Lunatic fringe promotes the lateral inhibition of neurogenesis**. *Development* 2009, **136**(15):2523-2533.
76. Amoyel M, Cheng YC, Jiang YJ, Wilkinson DG: **Wnt1 regulates neurogenesis and mediates lateral inhibition of boundary cell specification in the zebrafish hindbrain**. *Development* 2005, **132**(4):775-785.
77. Zhang D, Golubkov VS, Han W, Correa RG, Zhou Y, Lee S, Strongin AY, Dong PD: **Identification of Annexin A4 as a hepatopancreas factor involved in liver cell survival**. *Developmental biology* 2014, **395**(1):96-110.

Figure Legends

Figure 1: The Bacterial Artificial Chromosome reporter line *Tg(nkx6.1:eGFP)* mirrors the expression of the endogenous *nkx6.1* gene.

A-F: Immunodetection of endogenous Nkx6.1 (in red) and GFP (in green) in *Tg(nkx6.1:eGFP)* embryos of the indicated stages. Green arrows point to Nkx6.1-/GFP+ cells, red arrows to Nkx6.1+/GFP- cells. All views are either lateral (B, B' and C, C') or ventral (A, A'- and D, D'-F, F') with the anterior part to the left and represent either z-plane confocal images (B,D,E) or confocal projection images (A,C,F)**.** Scale bars = 30 µm. IPD: intra-pancreatic duct. EPD: extra-pancreatic duct, i: islet

Figure 2: *nkx6.1*-expressing cells gives rise to all pancreatic cell types.

A-D'': Immunodetection in 30hpf *Tg(nkx6.1:eGFP)* embryos of GFP with Isl1 (A-A''), Ins (B-B''), Sst (C-C'') or Gcg (D-D''). Yellow arrows point to cells coexpressing GFP and the respective hormones. **E-E'':** Fluorescent whole-mount *in situ* hybridization (WISH) of 55 hpf *Tg(nkx6.1:eGFP)* embryos using a *try* probe followed by GFP immunodetection. **F, F':** Immunodetection in 5 dpf *Tg(nkx6.1:eGFP)* embryos of GFP and of the hepato-pancreatic duct marker 2F11. **G-H':** Immunodetection of GFP and of Ins, Gcg and Sst hormones in 5 dpf *Tg(nkx6.1:eGFP)* embryos treated from 3 to 5 dpf with DMSO (G) or with the Notch signaling Inhibitor, LY411575 (H). Yellow arrows point to secondary endocrine GFP+/Hormones+ cells found in the IPD. All views are ventral with the anterior part to the left and represent either z-plane confocal images (A-E) or confocal projection images (F-H). Scale bars = 20 µm (A-E) or 40 µm (F-H).

Figure 3: *ascl1b*-expressing cells gives rise exclusively to endocrine cells of both dorsal and ventral bud.

A-E', H-I': Genetic lineage tracing using the *Cre-loxP system.* **A**: Schematic representation of the genetic lineage tracing experiments : the transgenic line *Tg(ascl1b:eGFP-creER^{T2})* was crossed with *the Tg(ubi:loxP-eGFP-loxP-mCherry)* line, abbreviated *Tg(ubi:Switch),* or with the *Tg(ubi:loxP-AmCyan-loxP-ZsYellow)* line, abbreviated *Tg(ubi:CSY),* treated with 4-hydro-tamoxifen (4OHT) at 11, 12, 13, 14 and 15 hpf (B-E') or at 13, 14 and 17 dpf (H-I') and fixed for analysis at the indicated times**.** Black triangles represent loxP sites. **B-E':** Immunodetection of CRE-mediated recombination markers (ZsYellow or mCherry, red) and Isl1 (B-B''), Ins (C-C''), Gcg (D-D'') or Nkx6.1 (E, E') in 4OHT treated embryos (green). Dotted white line delimitates the pancreas (E'). Yellow arrows point to cells co-expressing Rec

Marker (ZsYellow or mCherry) and the respective hormones (Ins or Gcg). **F-G':** Short-term lineage tracing: immunodetection of GFP and the Ins and Gcg hormones in 5 dpf *Tg(ascl1b:eGFP-creER^{T2})* embryos treated from 3 to 5 dpf with DMSO (F, F') or with the Notch Signaling Inhibitor LY411575 (G, G'). Yellow arrows in G' point to GFP+/Ins+/Gcg+ secondary endocrine cells found in the IPD. **H-I':** Immunodetection at 20 dpf of the CRE-mediated Rec Marker mCherry together with Ins and Gcg in 4OHT treated larvae. All views are ventral with the anterior part to the left and represent z-plane confocal images (B-D'') or confocal projection images (E-I'). Scale bars = 20 µm.

Figure 4: *nkx6.1* and *ascl1b* are first co-expressed in the endocrine precursors of the dorsal bud but rapidly their expression domain sets apart.

Immunodetection of endogenous Nkx6.1 and GFP in *Tg(ascl1b:eGFP-creER^{T2})* embryos at 14hpf (A-A'') and 15hpf (B-B''). All views are ventral with the anterior part to the left and represent confocal projection images**.** Scale bars = 40 µm. H: Hypochord, M: Medial Cells.

Figure 5: *ascl1b* and *nkx6.1* are regulated in an opposite way by Notch signaling pathway

A-F: WISH on wild-type (WT) embryos (A, C, E) or *mind bomb* (*mib$^{-/-}$*) mutants (B, D, F) with *ascl1b* (A-B) or *nkx6.1* (C-F) probes. Brackets delimitate the pancreatic domain. **G-H:** Immunodetection of GFP and endogenous Nkx6.1 in 5 dpf *Tg(ascl1b:eGFP-creER^{T2})* embryos treated from 3 to 5 dpf with DMSO (G) or with the Notch signaling inhibitor, LY411575 (H). **I-N:** WISH with *ascl1b* (I-J) or *nkx6.1* (K-L) probes or immunodetection of endogenous Nkx6.1 (M, N) of double-transgenic *Tg(hsp70:Gal4)* x *Tg(UAS:NICD)* embryos (J,L,N) or of control simple-transgenic embryos (I,K,M), both heat-shocked at 11 hpf during 20 min. Lateral views (A-F, K, L) or ventral views (G-J, M-N) of embryos of the indicated stages with the anterior to the left. Scale bars = 40 µm.

Figure 6: The pancreatic expression domain of Nkx6.1 includes the Notch-responsive cells.

Immunodetection of endogenous Nkx6.1 (red) and Venus (revealed with anti-GFP, green) in *Tg(TP1:VenusPest)* (A-C') or GFP in *Tg(Tp1:eGFP)* embryos (D-E') at the indicated stages. All views are ventral with the anterior part to the left and represent either z-plane confocal images (B-C') or confocal projection images (A, A', D, D', E, E'). Scale bars = 40 µm. IPD: intra-pancreatic duct. EPD: extra-pancreatic duct.

Figure 7: Expression of *nkx6.1* persists in duct cells in the adult pancreas

A and close-up A': GFP and Insulin (Ins, red) immunodetection on section through the pancreas of adult *Tg(nkx6.1:eGFP)* zebrafish. White arrows point to pancreatic ducts and asterisks show cells (presumably terminal end duct/centroacinar(CAC) cells dispersed throughout the exocrine tissue. A': close-up on an islet highlighted with Ins. **B:** Venus (green) and Ins (red) immunodetection in *Tg(Tp1:VenusPest)* showing the presence of Venus in CACs (asterisks) as previously reported [12], but not in duct cells within ductular structures (white arrow). Insets in A and B show isolated CAC. **C-D:** Immunodetection of Venus (green) and of endogenous Nkx6.1 (red) in *Tg(Tp1:VenusPest)* revealing co-labeling of both markers in CACs (C, C') while Nkx6.1 alone, but not Venus, labels the ducts. The white arrow in D points to a duct and asterisks indicate CACs. Dotted yellow lines delimitate the duct. **C'**: Same as C showing Nkx6.1 (red) and DAPI only. i: islet.

Figure 8: In the adult pancreas, Notch-responsive CACs give rise to other ductal and to endocrine cells and have the capacity to replicate.

Immunodetections on sections through the pancreas of adult *Tg(Tp1:VenusPest); Tg(Tp1:H2BmCherry).* **A:** Comparison of Venus (green) and H2BmCherry (red) labeling showing a small duct containing H2BmCherry+ cells that have lost Venus. **B:** Comparison of H2BmCherry (red) with the ductal marker 2F11 (green) showing some 2F11+ cells within a small duct co-expressing the stable H2BmCherry marker (yellow arrows). **C:** Weak H2BmCherry labeling near the extremity of a ductular structure (terminal, or intercalated duct) (yellow arrows); a CAC (intense H2BmCherry) at the tip of the terminal duct is indicated by an asterisk. **D and close-up D':** Some H2BmCherry+ cells, devoid of Venus (Notch off) co-express the beta cell marker Ins (white) (yellow arrows). Sections acquired in the head of the pancreas, at the level of the main endocrine islet. **E-E'** and **F-F':** Detection of EdU (red), Venus (green) and PCNA (white) in *Tg(Tp1:VenusPest)* adult fish injected with EdU. The pancreas was analyzed 20 hours (1 day post injection, dpi) (**E-E'**) and 5 days (dpi) (**F-F'**) after EdU injection.

Figure 9: nkx6.1:eGFP+ cells proliferate and differentiate into new Insulin-expressing cells after beta cell specific ablation.

GFP (green) and Ins (white) labeling in the pancreas of *Tg(nkx6.1:eGFP); Tg(ins:NTR-mCherry)* adult fish. (**A-B**) Non-treated fish (CTL, A) show intense Ins staining in beta cells, while Ins+ cells are not detected 3 days after treatment (dpt) with MTZ, indicating efficient ablation (B). Note that one beta cell debris (Ins+) is observed in the islet. (**C**) At 9 dpt Ins-expressing cells start to be detected in the principal islet and in extra-insular locations close to ductal GFP+ cells (yellow arrows). (**D**) At 21 dpt, islets show intense Ins staining consistent with beta cell recovery. (**E-G** and separate channels) While GFP is never detected

in beta cells of control fish (E), some regenerating Ins+ cells display weak GFP labeling at both stages of regeneration analyzed, i.e. at 9 dpt (F) and 21 dpt (G). (**H-I** and separate channels) Beta cell ablation triggers proliferation of CACs as shown at 3 dpt (**H**) compared to CTL (**I**) (asterisks). i: islet.

Figure 10. Expression of known pancreatic markers in the transcriptome of adult *nkx6.1*:eGFP cells.

Expression values are expressed as normalized counts. High expression of known ductal genes (orange box) is detected while acinar (green box) and endocrine (red box) markers display low abundance, with the exception of *pdx1* and *ascl1b* (see text).

Additional files

Additional file 1: Figure S1: The Bacterial Artificial Chromosome reporter line *Tg(nkx6.1:eGFP)* mirrors the expression of the endogenous *nkx6.1* gene.

A: Schematic representation of the −55 kb to +95 kb *nkx6.1:eGFP* BAC transgene. This BAC includes highly conserved sequence blocks amongst vertebrates (black boxes) located from 11kb to 77kb downstream of the *nkx6.1* gene. By BAC recombineering using galK selection, the *eGFP* cassette (green box) was introduced into the exon 1, replacing the beginning of the nkx6.1 open reading frame (aa 1 to 149). **B**: Epifluorescence microscopy images of the immunodetection of endogenous Nkx6.1 (red) and GFP (green) in *Tg(nkx6.1:eGFP)* embryos. Lateral views of 48 hpf embryos with the anterior part to the left. P: pancreas. **C**: Confocal projection images of whole mount fluorescent *in situ* hybridization on a *Tg(nkx6.1:eGFP)* embryo showing that the *gfp* transcripts are not expressed in the *Insulin*+ cells at 20 hpf.**D**: Confocal projection images of whole mount fluorescent *in situ* hybridization on a *Tg(nkx6.1:eGFP)* embryo showing that the *gfp* transcripts are not expressed in the *isl1*+ cells at 30 hpf. C-C'' and D-D'': Scale bar = 15 µm.

Format: PNG Size: 2.55 MB

Additional file 2: Figure S2: The Bacterial Artificial Chromosome reporter line *Tg (ascl1b:eGFP-creER^{T2})* mirrors the expression of the endogenous *ascl1b* gene.

A: Schematic representation of the −61 kb to +89 kb *ascl1b:eGFP-2A-creER^{T2}* BAC transgene. By BAC recombineering using galK selection, the *eGFP-2A-creER^{T2}*cassette is introduced into the exon 1, replacing the beginning of the *ascl1b* open reading frame (aa 1 to 163). **B**: Epifluorescence microscopy images of the immunodetection of GFP in 17 hpf

*Tg(ascl1b:eGFP-creER^{T2})*embryos. **C-D:** Visible WISH showing expression of endogenous *ascl1b* in WT embryo(C) and of *GFP* in *Tg(ascl1b:eGFP-creER^{T2})* embryos (D) at 15hpf. Lateral views with the anterior part to the left. P: pancreas.
Format: PNG Size: 1.04 MB

Additional file 3: Figure S3: *nkx6.1* expression is not repressed by Ascl1b.
A: Schematic representation of WT and mutant Ascl1b$^{ulg\text{-}M2C}$ protein. The basic domain (b) (+70/+78) is represented by a blue box and the helix loop helix (HLH) domain (+79/+123) by a green box. The coding region of the mutant Ascl1b$^{ulg\text{-}M2C}$ protein contains a 11 pb deletion after the aa107 codon, leading to a frameshift and the production of an aberrant region of 48 aa instead of the second helix, known to be essential for the function of the bHLH proteins. **A':** Table showing part of the nucleotide and protein sequence of the *ascl1b* gene and of the mutated form in the Ascl1b$^{ulg\text{-}M2C}$ mutant. **B-C:** WISH showing the drastic reduction of somatostatin expression in ascl1b$^{-/-}$ mutant compared to the WT embryo at 30hpf. This phenotype is identical to the one of embryos injected with a translation-blocking morpholino, targeting the translation start site of ascl1b mRNA [15, 75, 76], suggesting that the mutant Ascl1b$^{ulg\text{-}M2C}$ is effectively a null mutant. **(D-E)** Confocal projection images of Nkx6.1 immunodetection showing equivalent number of nkx6.1+ cells in WT and *ascl1b$^{-/-}$* mutant at 16 hpf. All views are ventral with the anterior part to the left. Scale bars = 40 µm.
Format: PNG Size 1.28 MB

Additional file 4: Figure S4: *ascl1b* expression is not repressed by Nkx6.1
A: Schematic representation of WT and mutant Nkx6.1$^{ulg\text{-}M5}$ protein with the yellow box representing the homeodomain and red box representing the NK domain. The coding region of the mutant Nkx6.1$^{ulg\text{-}M5}$ protein contains a 7 bp deletion after the aa 141 codon, leading to the apparition of a STOP codon just after the deletion. The black line represents the region of the protein recognized by the Nkx6.1 antibody**. A':** Table showing part of the nucleotide and protein sequence of the nkx6.1 gene and of the mutated form in the Nkx6.1$^{ulg\text{-}M5}$ mutant. **B-C:** Nkx6.1 immunodetection showing the loss of the full length Nkx6.1 protein in the *nkx6.1$^{-/-}$* mutant. **D-E:** Glucagon immunodetection showing a drastic reduction of the number of glucagon expressing cells in *nkx6.1$^{-/-}$* mutant compared to the WT embryo at 30 hpf. This phenotype is the same as the one of embryos injected with the MO1 *translation*-blocking *morpholino,* targeting the translation start site of *nkx6.1* mRNA [18], shown to efficiently prevent *nkx6.1* expression in the neural tube [70]. This strongly suggests that the mutant Nkx6.1$^{ulg\text{-}M5}$ is a null mutant. **F-G:** Confocal projection images of fluorescent WISH

showing equivalent number of *ascl1b*+ cells in WT and *nkx6.1*$^{-/-}$ mutant at 15 hpf. All views are ventral with the anterior part to the left. Scale bars = 40 µM.
Format: PNG Size 1.47 MB

Additional file 5: Figure S5: The initiation of *nkx6.1* expression is independent of Notch signaling

A-D: Fluorescent WISH showing a drastic increase in the pancreatic dorsal bud of *ascl1b* expression in the *mind bomb(mib*$^{-/-}$*)* mutants while *nkx6.1* expression is not affected at 13 hpf. **E-F:** Fluorescent WISH showing that the pancreatic expression of *nkx6.1* in the ventral bud is not perturbed at 34hpf in *mib*$^{-/-}$ mutants. The ventral (A-B, E-F) or lateral (C-D) views represent confocal projection images with the anterior to the left. Scale bars = 40 µM. NS, Nervous system.
Format: PNG Size 971 Ko

Additional file 6: Figure S6. All Notch-responsive cells in the adult pancreas are CACs

Notch active cells in *Tg(Tp1:VenusPest)* adult fish were labeled with anti-GFP to visualize VenusPest(green) and the ductal marker 2F11 (red). VenusPest labeling is detected throughout the exocrine tissue (see asterisks highlighting examples) and where it highlights the CACs together with 2F11. In contrast, ductal structures with intense 2F11 staining do not exhibit any Venus+ (Notch ON) cells. Note also the presence of 2F11 in endocrine islet cells as previously reported [77].
Format: PNG Size 2.78 MB

Additional file 7: Figure S7: Notch-responsive terminal end duct cells/CACs give rise to other ductal cells.

Immunodetection of H2BmCherry and ductal markers in the pancreas of adult *Tg(Tp1:VenusPest); Tg(Tp1:H2BmCherry)* zebrafish. **A-C:** H2BmCherry+ cells (red) in ductular structures labeled with the ductal (ducts and CACs) marker 2F11 (green). **A-B**: separate channels of Figure 8B-C. **B-C:**Weak H2BmCherry labeling is present near the extremity of a terminal (or intercalated) duct (yellow arrows). The asterisk identifies a CAC at the tip of the duct (strong H2BmCherry labeling). **D:** Comparison of H2BmCherry (red) with endogenous Nkx6.1 (green) showing ductal Nkx6.1+ cells co-expressing H2BmCherry (yellow arrows).
Format: PNG Size 4.85 MB

Additional file 8: Supplemental Table 1 : Duct-specific genes

Duct-specific genes listed by decreased expression level. 293 genes were found corresponding to the following "specificity" criteria :
- gene expression level >1000 normalized counts in duct AND <1000 in non ductal (averaged endocrine and acinar) transcriptome.
- ≥16 fold enrichment in ducts versus non duct (averaged endocrine and acinar), expressed in log2 ratio (≥4).
Ratio = mean of normalized counts in duct transcriptomes / mean of normalized counts in endocrine and in acinar transcriptomes.
Known ductal markers and genes involved in the Notch pathway are highlighted in red. Novel markers and genes involved in the Wnt pathway are highlighted in green.
Format: DOCX Size 26.2 Ko

Additional file 9: Figure S8: Ductal expression of *id2a* during zebrafish development.
Whole mount fluorescent *in situ* hybridization showing *id2a* (green) and the ductal marker *sox9b* (red) in a 3 dpf larva. The expression of both genes overlaps as highlighted by yellow labeling. In addition to expression in the intrapancreatic ducts (IPD), *id2a* is also expressed in the intrahepatic (IHD). HPD: hepatopancreatic ducts.
Format PNG Size: 536 Ko

Additional file 10: Supplemental Table 2 : List of the primers used in this study.
The 50 nucleotides added to allow homologous recombination are indicated in capital.
Format: DOCX SIze: 12.9 Ko

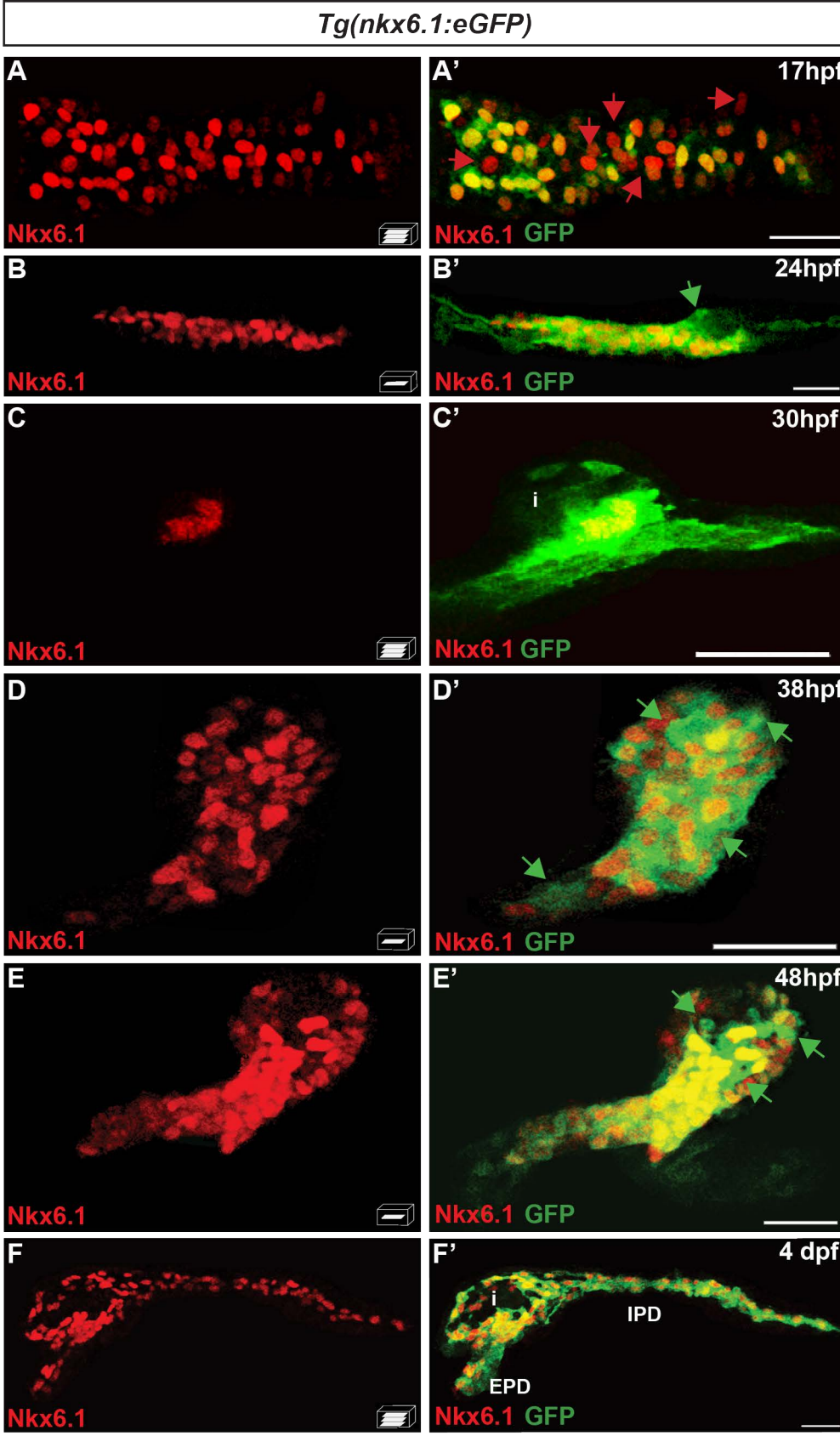
Tg(nkx6.1:eGFP)
A
Nkx6.1
A'
17hpf
Nkx6.1 GFP
B
Nkx6.1
B'
24hpf
Nkx6.1 GFP
C
Nkx6.1
C'
30hpf
i
Nkx6.1 GFP
D
Nkx6.1
D'
38hpf
Nkx6.1 GFP
E
Nkx6.1
E'
48hpf
Nkx6.1 GFP
F
Nkx6.1
F'
4 dpf
i
IPD
EPD
Nkx6.1 GFP

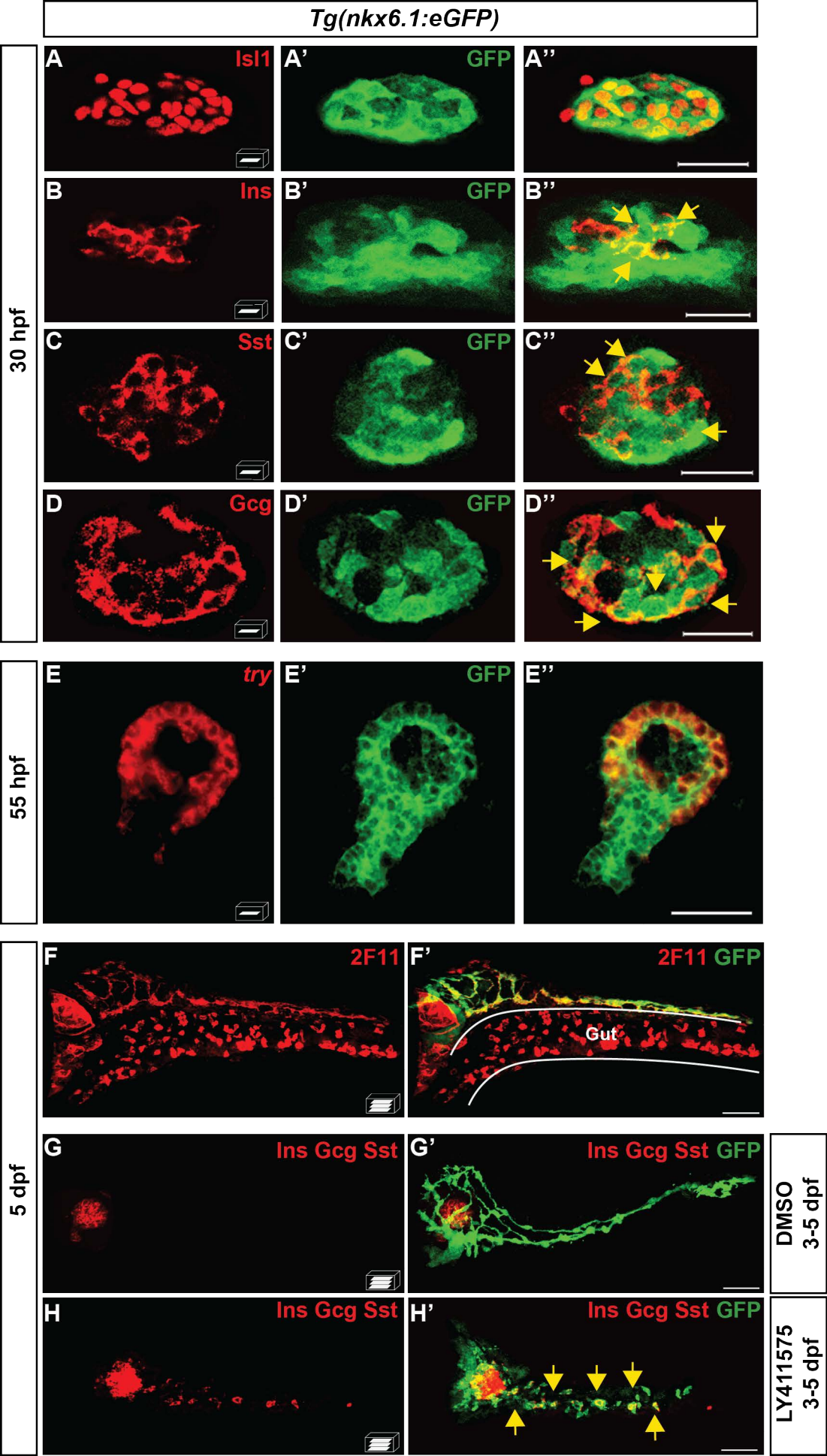
Tg(nkx6.1:eGFP)
30 hpf
A
Isl1
A'
GFP
A''
B
Ins
B'
GFP
B''
C
Sst
C'
GFP
C''
D
Gcg
D'
GFP
D''
55 hpf
E
try
E'
GFP
E''
5 dpf
F
2F11
F'
2F11 GFP
Gut
G
Ins Gcg Sst
G'
Ins Gcg Sst GFP
DMSO
3-5 dpf
H
Ins Gcg Sst
H'
Ins Gcg Sst GFP
LY411575
3-5 dpf

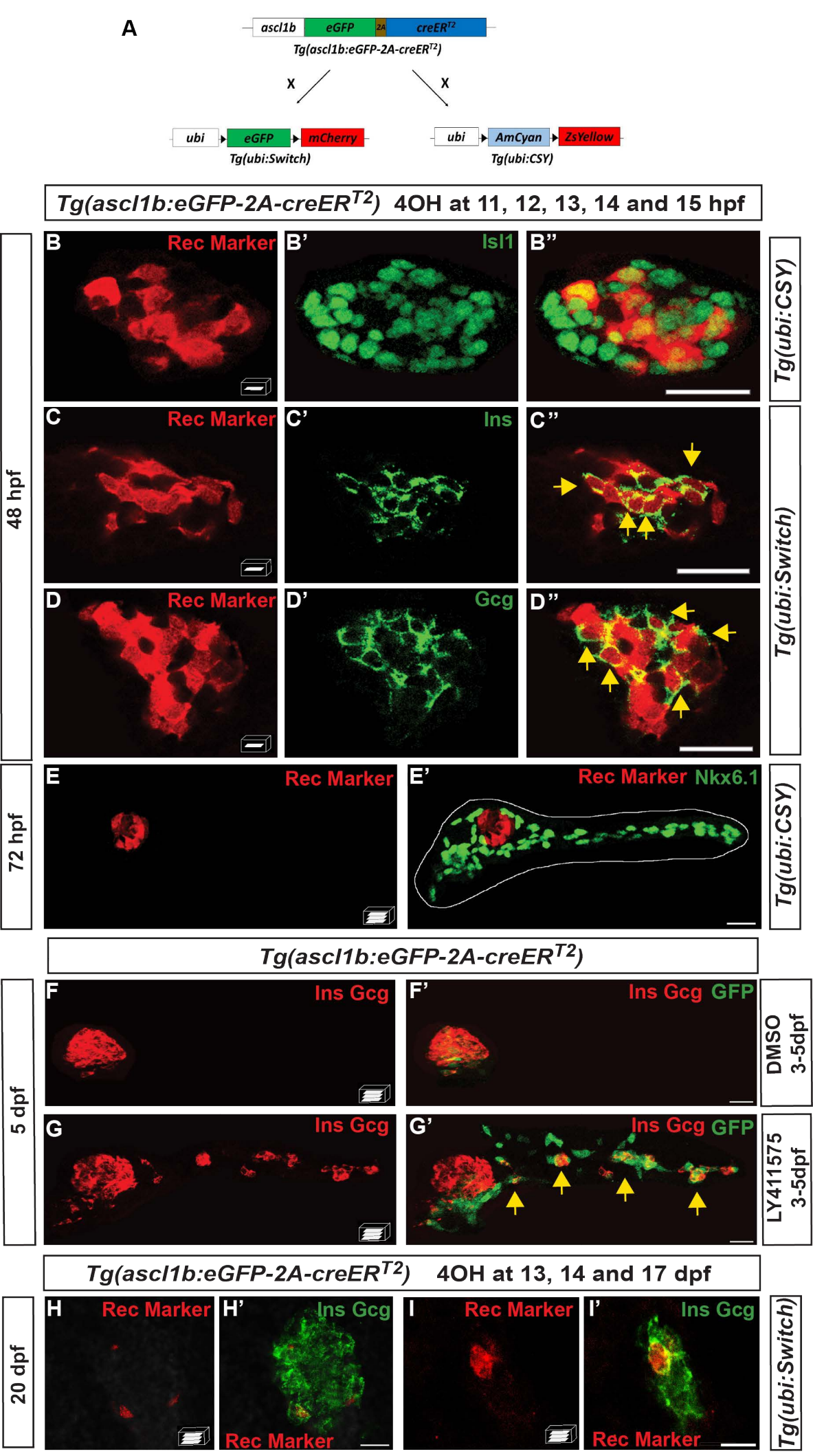
A
ascl1b
eGFP
2A
creER^T2
Tg(ascl1b:eGFP-2A-creER^T2)
X
X
ubi
eGFP
mCherry
Tg(ubi:Switch)
ubi
AmCyan
ZsYellow
Tg(ubi:CSY)
Tg(ascl1b:eGFP-2A-creER^T2) 4OH at 11, 12, 13, 14 and 15 hpf
48 hpf
B Rec Marker
B' Isl1
B" Tg(ubi:CSY)
C Rec Marker
C' Ins
C" Tg(ubi:Switch)
D Rec Marker
D' Gcg
D"
72 hpf
E Rec Marker
E' Rec Marker Nkx6.1
Tg(ubi:CSY)
Tg(ascl1b:eGFP-2A-creER^T2)
5 dpf
F Ins Gcg
F' Ins Gcg GFP
DMSO 3-5dpf
G Ins Gcg
G' Ins Gcg GFP
LY411575 3-5dpf
Tg(ascl1b:eGFP-2A-creER^T2) 4OH at 13, 14 and 17 dpf
20 dpf
H Rec Marker
H' Ins Gcg
Rec Marker
I Rec Marker
I' Ins Gcg
Rec Marker
Tg(ubi:Switch)

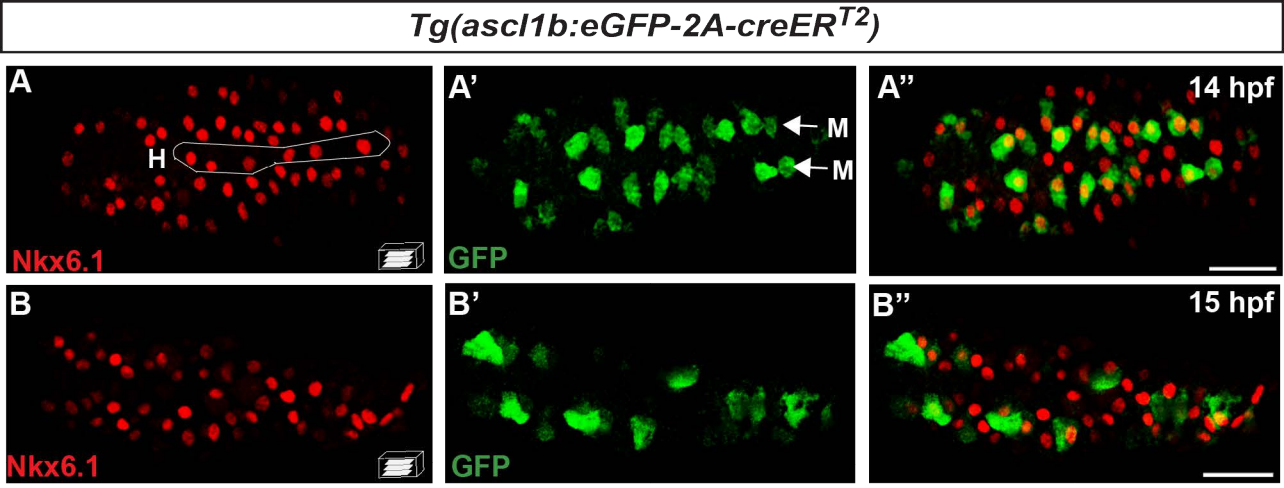
Tg(ascl1b:eGFP-2A-creER^{T2})
A
H
Nkx6.1
A'
M
M
GFP
A''
14 hpf
B
Nkx6.1
B'
GFP
B''
15 hpf

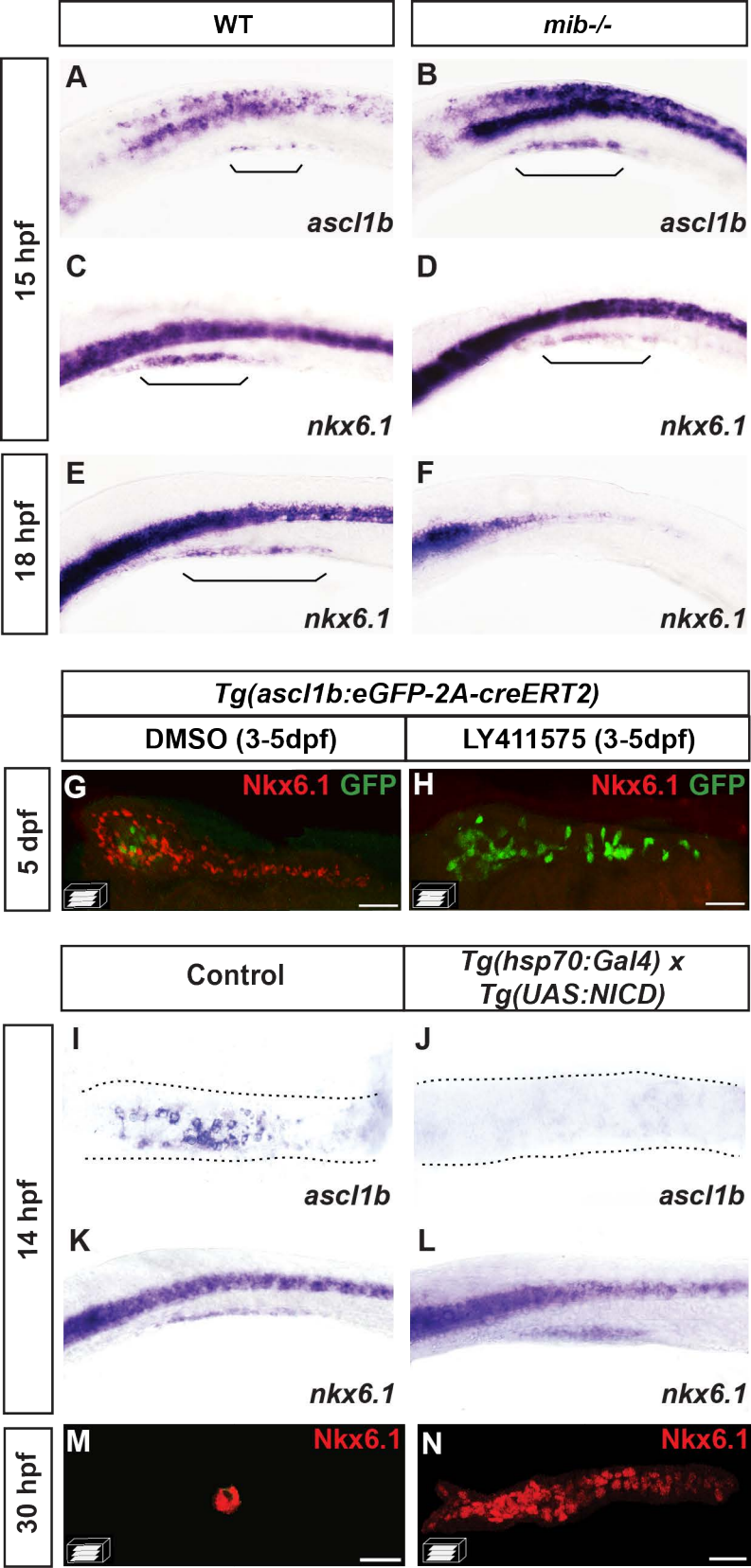
WT
mib-/-
15 hpf
A
ascl1b
B
ascl1b
C
nkx6.1
D
nkx6.1
18 hpf
E
nkx6.1
F
nkx6.1
Tg(ascl1b:eGFP-2A-creERT2)
DMSO (3-5dpf)
LY411575 (3-5dpf)
5 dpf
G
Nkx6.1 GFP
H
Nkx6.1 GFP
Control
Tg(hsp70:Gal4) x Tg(UAS:NICD)
14 hpf
I
ascl1b
J
ascl1b
K
nkx6.1
L
nkx6.1
30 hpf
M
Nkx6.1
N
Nkx6.1

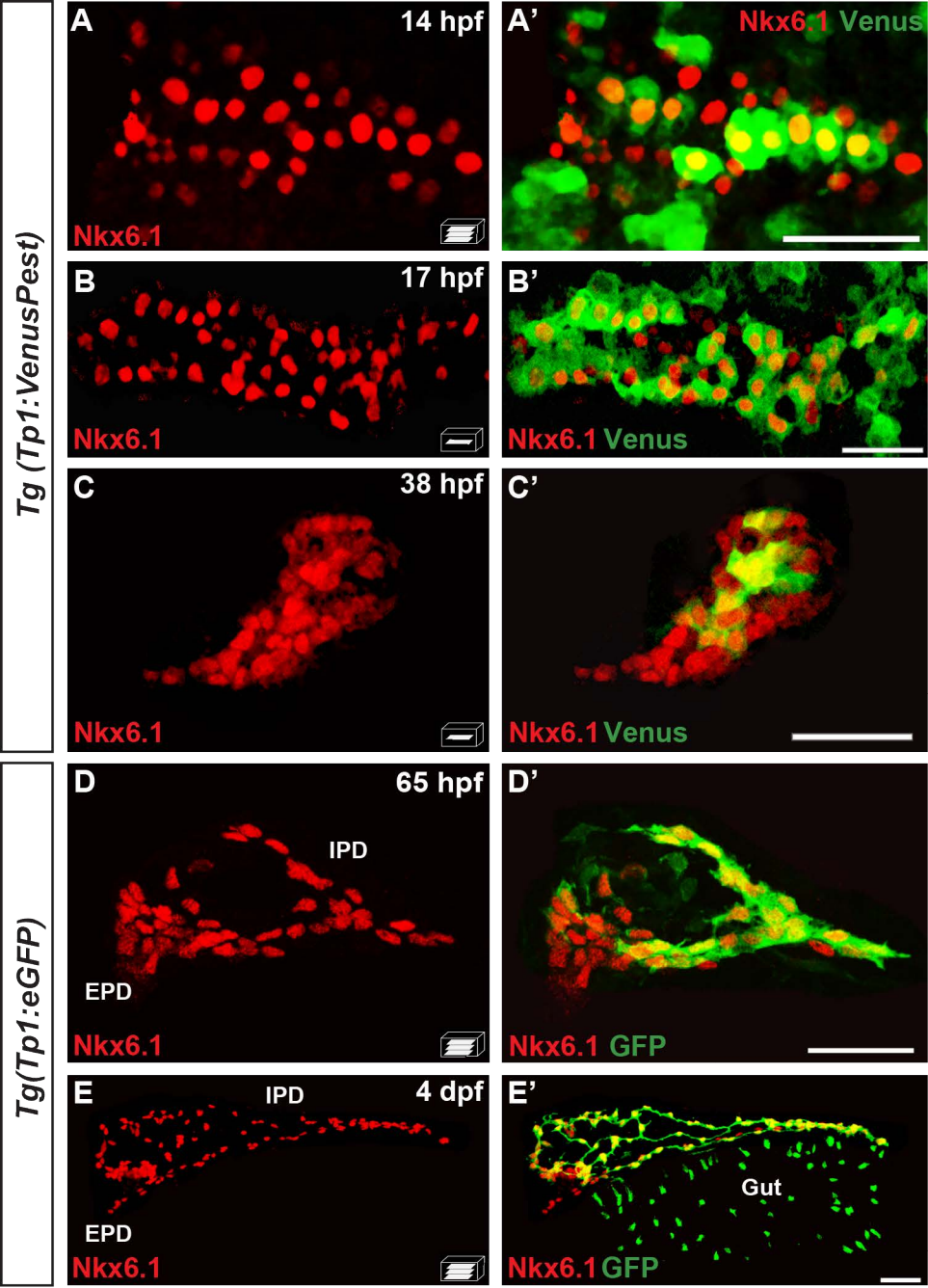
Tg (Tp1:VenusPest)
A
14 hpf
Nkx6.1
A'
Nkx6.1 Venus
B
17 hpf
Nkx6.1
B'
Nkx6.1 Venus
C
38 hpf
Nkx6.1
C'
Nkx6.1 Venus
Tg(Tp1:eGFP)
D
65 hpf
IPD
EPD
Nkx6.1
D'
Nkx6.1 GFP
E
IPD
4 dpf
EPD
Nkx6.1
E'
Gut
Nkx6.1 GFP

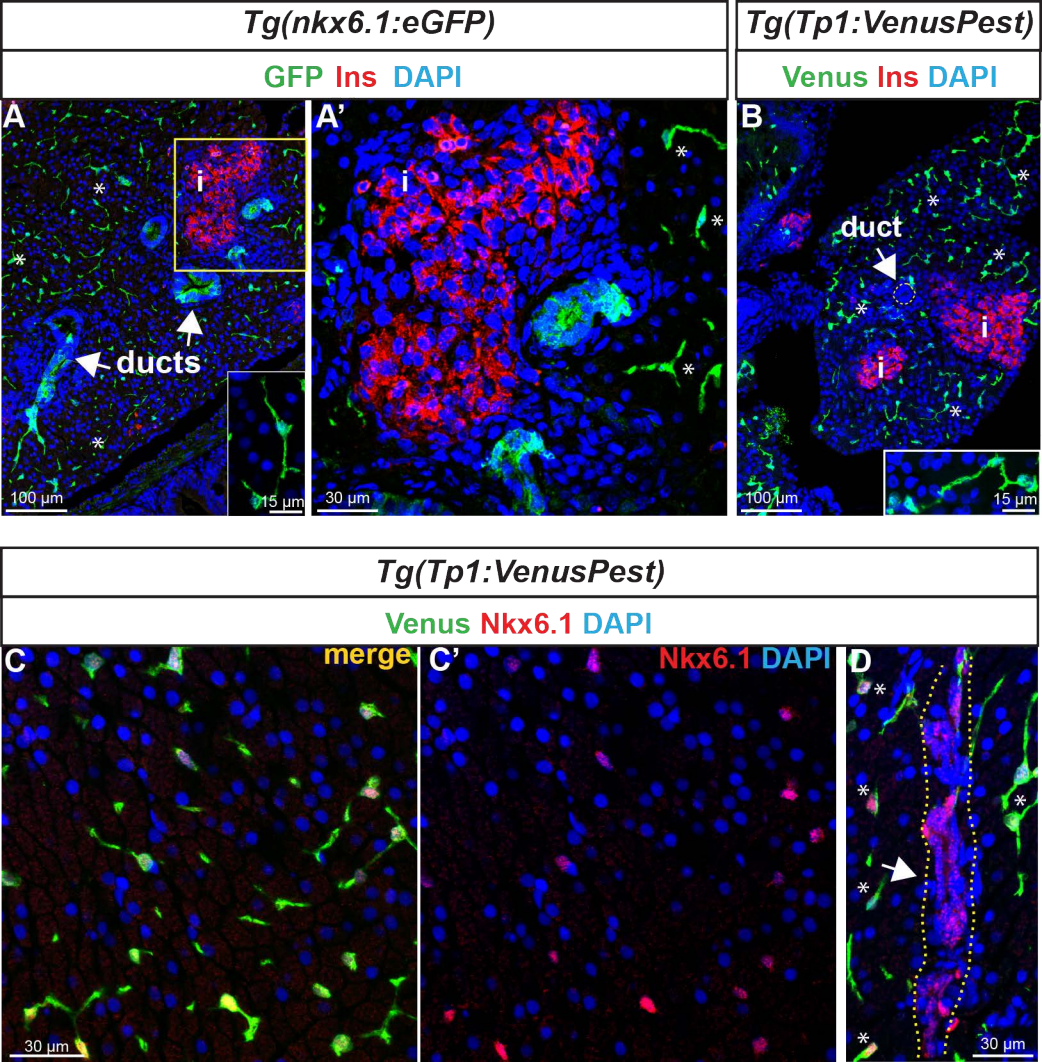
Tg(nkx6.1:eGFP)
GFP Ins DAPI
Tg(Tp1:VenusPest)
Venus Ins DAPI
A
A'
B
i
ducts
duct
100 µm
15 µm
30 µm
Tg(Tp1:VenusPest)
Venus Nkx6.1 DAPI
C
merge
C'
Nkx6.1 DAPI
D
30 µm

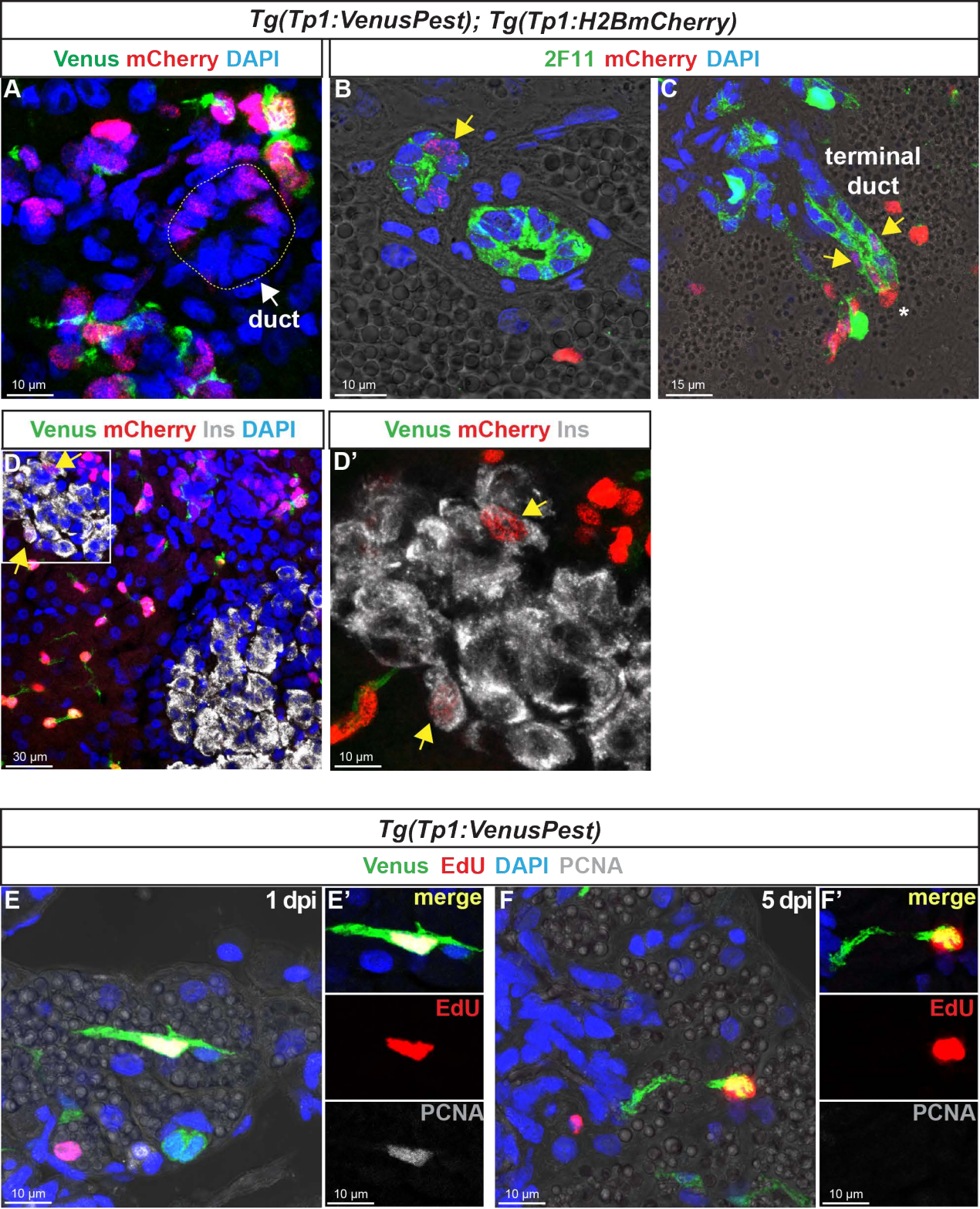
Tg(Tp1:VenusPest); Tg(Tp1:H2BmCherry)
Venus mCherry DAPI
2F11 mCherry DAPI
A
duct
10 µm
B
10 µm
C
terminal duct
*
15 µm
Venus mCherry Ins DAPI
D
30 µm
Venus mCherry Ins
D'
10 µm
Tg(Tp1:VenusPest)
Venus EdU DAPI PCNA
E
1 dpi
10 µm
E'
merge
EdU
PCNA
10 µm
F
5 dpi
10 µm
F'
merge
EdU
PCNA
10 µm

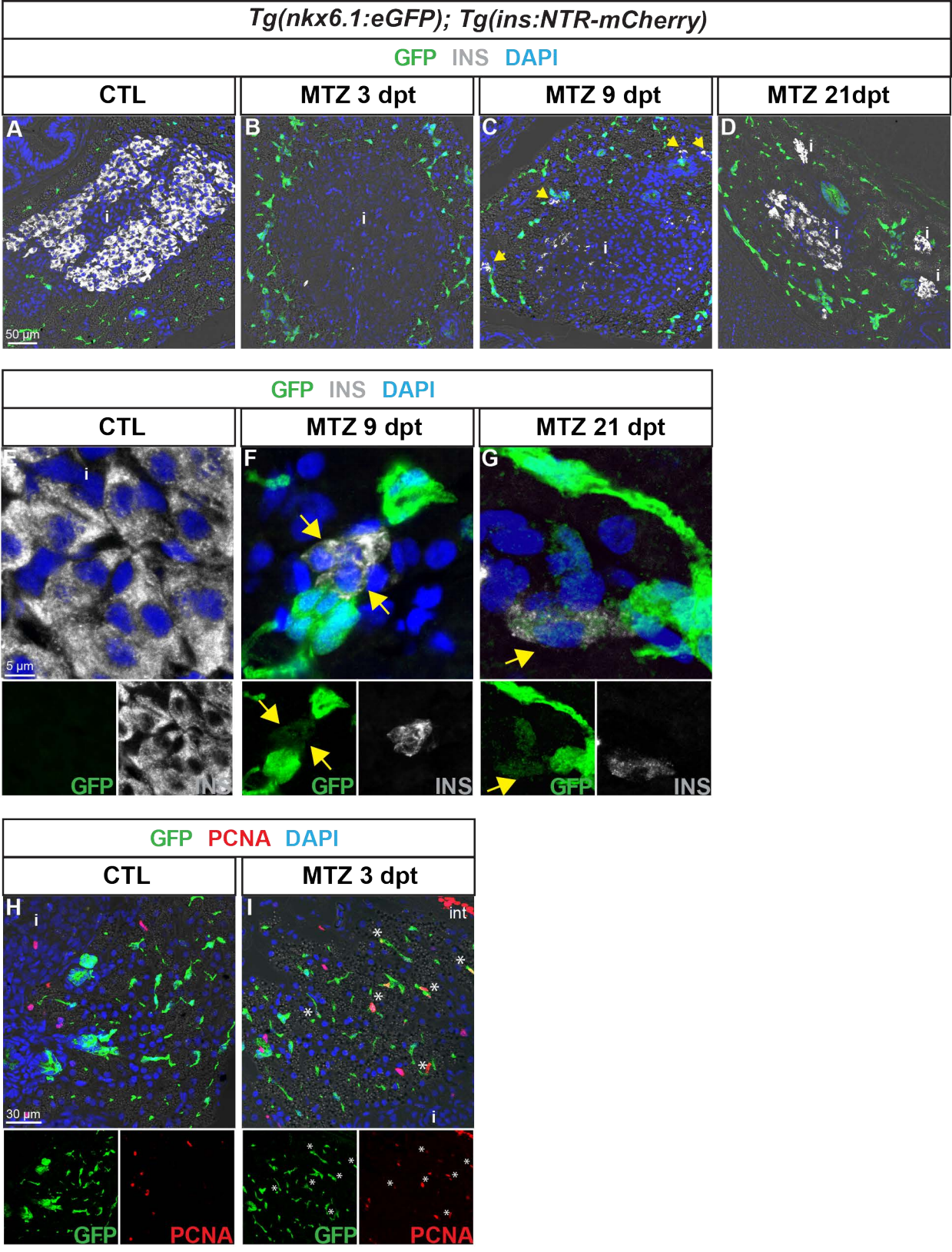
Tg(nkx6.1:eGFP); Tg(ins:NTR-mCherry)
GFP INS DAPI
CTL
MTZ 3 dpt
MTZ 9 dpt
MTZ 21dpt
A
B
C
D
i
50 µm
GFP INS DAPI
CTL
MTZ 9 dpt
MTZ 21 dpt
E
F
G
5 µm
GFP
INS
GFP PCNA DAPI
CTL
MTZ 3 dpt
H
I
int
30 µm
PCNA

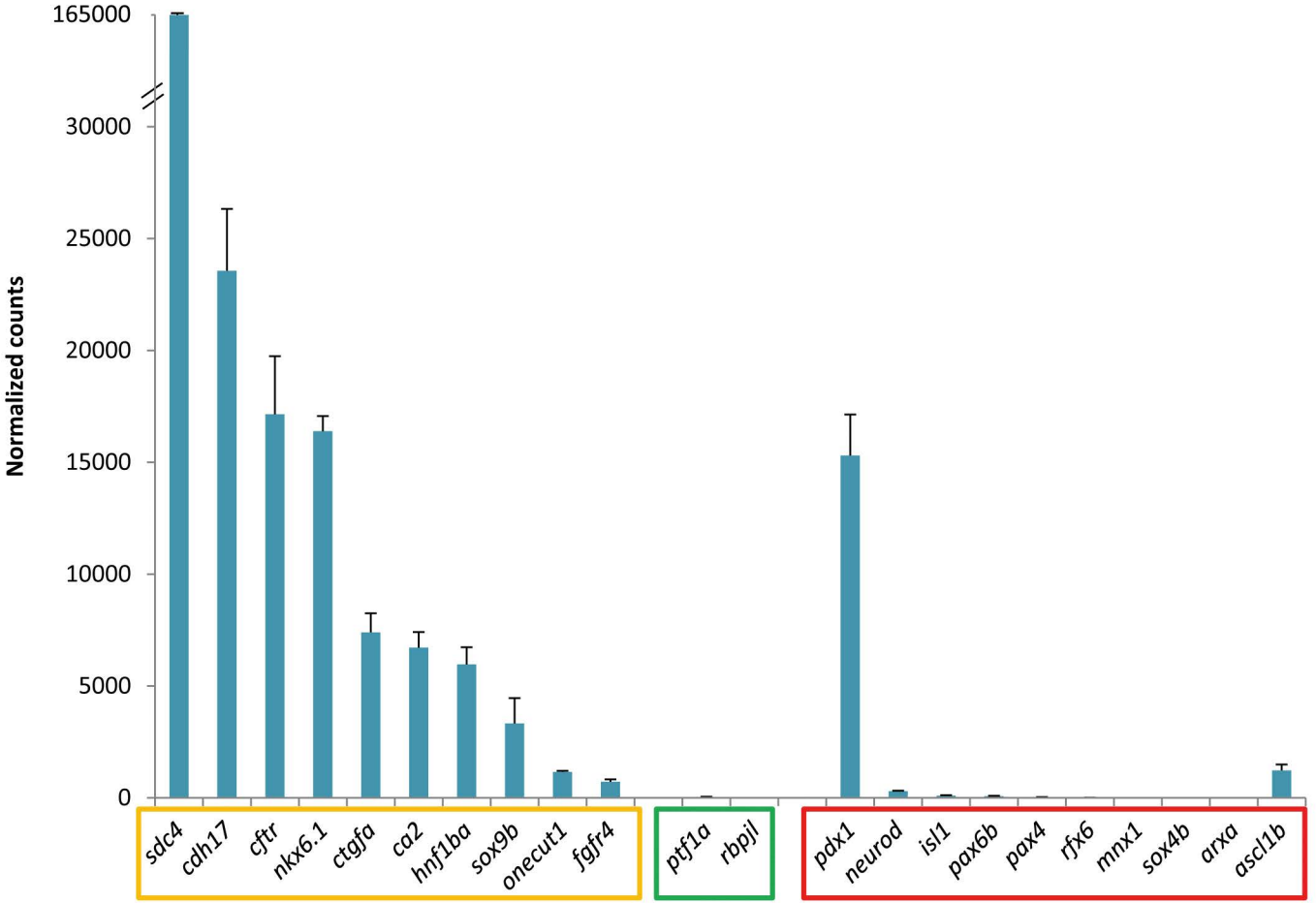
Normalized counts
165000
30000
25000
20000
15000
10000
5000
0
sdc4
cdh17
cftr
nkx6.1
ctgfa
ca2
hnf1ba
sox9b
onecut1
fgfr4
ptf1a
rbpjl
pdx1
neurod
isl1
pax6b
pax4
rfx6
mnx1
sox4b
arxa
ascl1b